

Reactivity of Individual Organolithium Aggregates – a RINMR Study of *n*-Butyllithium and 2-Methoxy-6-(methoxymethyl)phenyllithium

Amanda C. Jones, Aaron W. Sanders, Martin J. Bevan, and Hans J. Reich,*
Department of Chemistry, University of Wisconsin Madison, WI 53706

Supporting Information

Table of Contents

S1. Rapid Injection NMR Experiment

Introduction	S-3
The Rapid Injection Apparatus	S-4
Temperature Control	S-9
Volume Accuracy of Injection	S-10
Normal/Inverse Mode of Injection	S-10
Low Temperature Experiments	S-11
Saturation	S-11
Accuracy of Timing	S-12
Air/Water Problem	S-12
General Procedure for a RINMR Experiment	S-13
Spectrometer Control of the Injector	S-13
Pulse Program for Proton or Lithium Kinetics Runs	S-14

S2. General Experimental	S-18
------------------------------------	------

S3. Syntheses

deutero-(Trimethylsilyl)acetylene (<i>d</i> -1a)	S-19
(Trimethylsilyl)phenylthioethyne	S-19
(Phenylthio)acetylene (1c)	S-19
Reaction of <i>n</i> -BuLi with Aldehydes	S-19
1-Phenyl-1-pentanol	S-20
1-(4-Diethylaminophenyl)-1-pentanol	S-20
3-Methoxymethylanisole	S-20
2-Trimethylstannyl-3-methoxymethyl-anisole	S-20

S4. Competition Kinetics

Competition Experiments with <i>n</i> -BuLi	S-21
Competition Experiments with 2-Methoxy-6-(methoxymethyl)phenyllithium (5)	S-21
Propargyl Alcohols (6a-c)	S-21
1-Phenyl-3-(trimethylsilyl)prop-2-yn-1-ol (6a)	S-22
1-Phenyl-3-(triphenylsilyl)prop-2-yn-1-ol (6b)	S-22
1-Phenyl-3-(phenylthio)prop-2-yn-1-ol (6c)	S-22

S5. NMR Characterization of Lithium Reagents

Product Lithium Acetylides (<i>d</i> -4a)	S-23
Recrystallization of 2-Methoxy-6-(methoxymethyl)phenyllithium (5)	S-25
Characterization of 2-Methoxy-6-methoxymethylphenyllithium (5)	S-25

S6. Rapid Injection NMR Kinetics

Preparation <i>n</i> -BuLi Samples	S-27
Kinetic Simulations	S-27
Reactivity of <i>n</i> -BuLi with (Trimethylsilyl)acetylene (1a)	S-27
Reactivity of <i>n</i> -BuLi with deutero-(Trimethylsilyl)acetylene (<i>d</i> -1a)	S-29

Disproportionation of the Mixed Dimer (3a)	S-31
Reactivity of (<i>n</i> -BuLi) ₄ with (Phenylthio)acetylene (1c)	S-32
Reactivity of (<i>n</i> -BuLi) ₄ with Benzaldehyde	S-33
Reactivity of (<i>n</i> BuLi) ₄ with <i>p</i> -Diethylaminobenzaldehyde	S-34
Reactivity of 2-Methoxy-6-(methoxymethyl)phenyllithium (5)	S-35
S8. References Supporting Information	S-37

S1. The Rapid Injection NMR Experimental Setup

Introduction. Several research groups have deployed rapid injection NMR (RINMR) apparatus,^[S-1, S-2a, S-3-S-8] for the study of fast organometallic reactions at low temperature. Most are based on a design reported by McGarrity, Ogle and Loosli,^[S-1] which employs a piston-driven syringe suspended above the NMR tube inside the bore of the spectrometer magnet. A special nozzle on the tip of the syringe needle (which is dipped into the NMR sample) causes turbulent mixing of the sample from a vigorous injection. Although very short time scale experiments were reported for such an apparatus (less than 100 msec), no experiments below -95 °C were reported, presumably because solvent viscosity at lower temperatures makes injection-induced turbulent mixing impractical, and perhaps because cooling of the syringe, which is mounted in the cooling gas stream, may cause malfunctions. We were interested in a simpler and more robust design (related to one developed by the group at Erlangen^[S-2a]), in which syringes are mounted above the spectrometer, with the sample being injected into the NMR tube through a long teflon needle. This makes it possible to carry out more than one injection (our apparatus has two syringe mounts). More importantly, it allows the use of a mechanical stirrer mounted above the spectrometer magnet so that efficient mixing can be achieved at any temperature consistent with solvent freezing point and sample solubility. Our apparatus was constructed to operate with 10 mm NMR tubes, since we were planning multinuclear NMR experiments where sensitivity was an important issue. Larger sample size also leads to more precision in volume and concentration measurements. Although it may be feasible to work with smaller tubes, the space constraints in the NMR tube would require more delicate stirring and injection components, and we did not attempt to construct one.

The ability to execute RINMR experiments at very low temperatures on a time scale of a few seconds is a crucial aspect of our apparatus. For example, McGarrity, Ogle and Loosli^[S-1b] studied the reactivity of the dimer and tetramer of *n*-BuLi at -85 °C, where the half-life of the tetramer is approximately 2.5 seconds. This makes it difficult to study the aggregates independently, since the time scale of interconversion is comparable to both T_1 of the observed nuclei and the acquisition time of the FID. In the experiments reported in this paper at -130 °C, the half-life of the (*n*-BuLi)₄ - (*n*-BuLi)₂ interconversion is approximately one hour, so that experiments to individually measure the reactivity of the two aggregates have a very large dynamic range. A more quantitative depiction is given in Fig. S-1, which shows the “Curtin-Hammett” line for a 15-second time-scale kinetic study. For ΔG^\ddagger values below the line, individual species are interconverting on the time scale of the experiment, and the Curtin-Hammett principle applies. Above the line, the reactivity of the species can be individually measured, since they are interconverting slower than the rate of reaction. For a successful experiment, the interconversion barrier must be well (1-2 kcal/mol) above the barrier for reaction, and both must also be above the line. At -85 °C the activation energy for species interconversion must be >12 kcal/mol for a 15-sec time-scale experiment to provide useful information, whereas at -135 °C, reactions can be studied under non-Curtin-Hammett conditions if the species interconvert with activation energies of ≥ 9 kcal/mol. Thus, measurement of the reactivity of *n*-BuLi dimer and tetramer (ΔG^\ddagger_{-84} for interconversion ca 11.4 kcal/mol) is marginal at best at -84 °C, but can be done readily at -135 °C. The problem of working too close to the “Curtin-Hammett line” is illustrated by one of the conclusions of McGarrity, Ogle and Loosli: that the dimer is ca 10 times as reactive as the tetramer towards benzaldehyde, a number which we now know to be too small by at least 3 orders of magnitude.

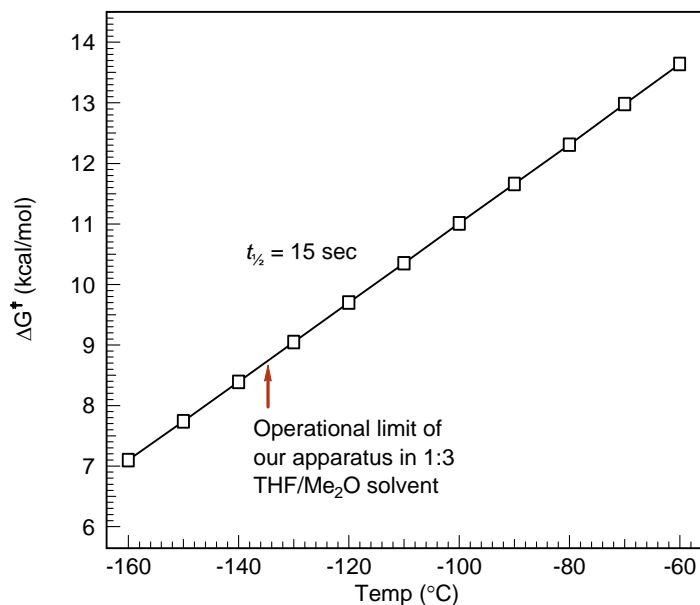


Figure S-1. Relationship between temperature and activation energy for a reaction with a 15 s half-life. If two species are present, both of which could participate in the reaction, their barrier to interconversion must be well above the line for the rates to be independently measurable with our apparatus.

The Rapid Injection Apparatus. The automatic RINMR device that we built (Fig. S-2) consists of the following parts, which are assembled for use directly above the spectrometer magnet (a Bruker Avance 360 MHz spectrometer):

1. The main body of the injector consists of a fixed part (FRAME), and a moving part (CARRIAGE). On the FRAME are mounted a pneumatic cylinder to move the CARRIAGE, air valves for the pneumatic cylinders, and two brass guide rails. The CARRIAGE slides on the brass rails, and serves to lower and raise the stirrer and injection needle(s) into and out of the NMR sample. On the CARRIAGE are mounted the syringe(s), pneumatic cylinders for activating the syringes, and the stirring motor. The FRAME (2 kg) and CARRIAGE (3 kg) are deliberately massive to help absorb the shock of injection and spring return. The FRAME is fastened to the ceiling, with the stirrer shaft centered above the spectrometer magnet bore.

2. The INSERT is placed inside the magnet bore and provides a guide to position needle(s) and stirrer shaft in the magnet bore and into the top of the 10 mm NMR tube. It is attached to the CARRIAGE via guide adapter (E) and moves up and down with it.

3. The electronic control panel (CONTROLLER) provides control of the movement of the injection CARRIAGE, the stirrer, and the pneumatic cylinders which actuate the syringe(s). It can be operated manually, or by the pulse program.

4. The SCAFFOLD (optional) provides protection for the top of the spectrometer magnet. It is basically a holder for the INSERT. This is the only part of the apparatus that touches the spectrometer.

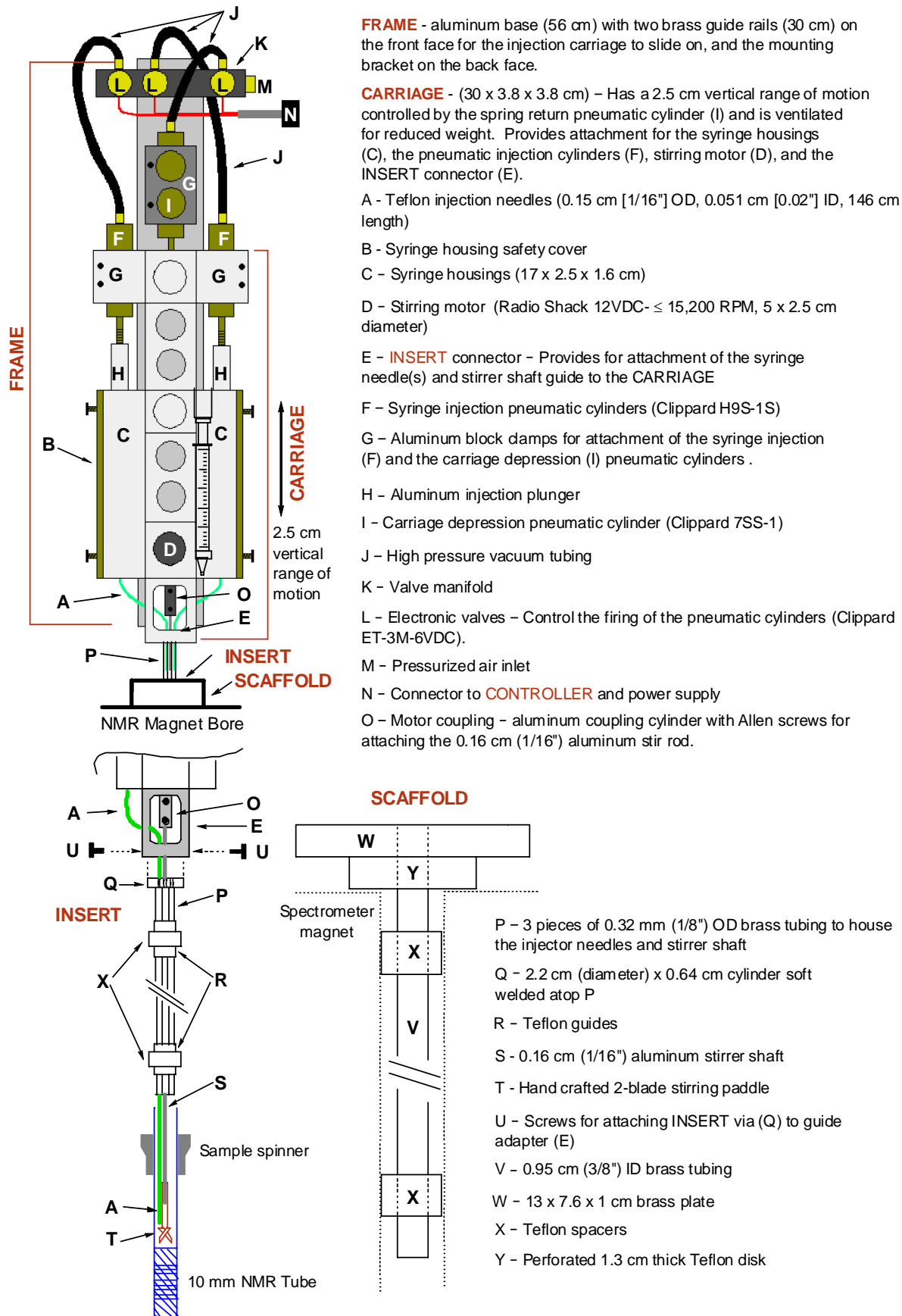


Figure S-2. Schematic of the injector apparatus.

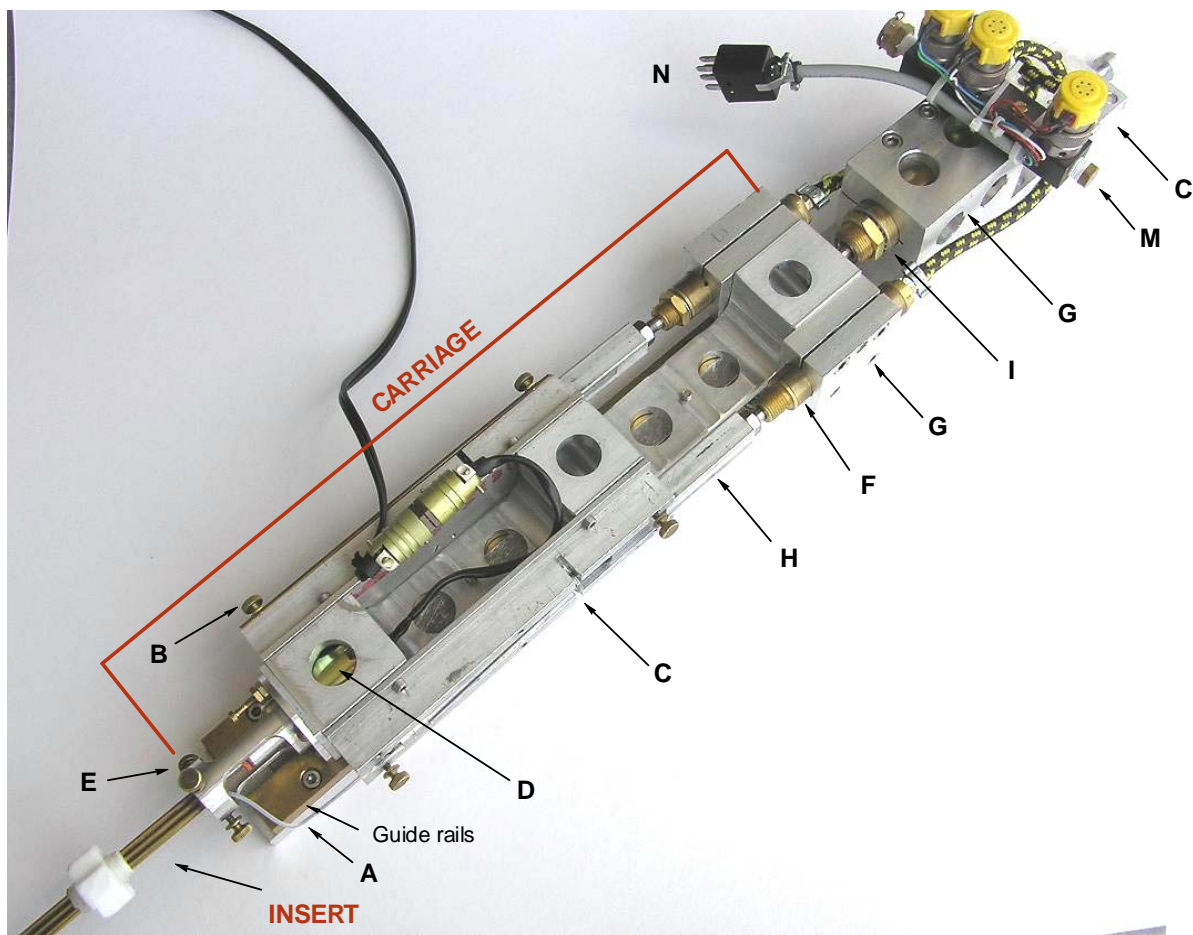


Figure S-3. Photograph of the injection apparatus.

The FRAME consists of a 56 x 5 x 0.8 cm aluminum base. On the back of the base is an aluminum fitting (Fig. S-4b) which slides into a matching fitting permanently mounted to the ceiling above the spectrometer magnet. At the top of the base is mounted an aluminum clamp (G) for the main pneumatic cylinder (Clippard 7/8" (2.2 cm) Bore, Brass Heavy Duty Minimatic Cylinder with Single Acting Spring Return and Stud mount, 7SS-1) which actuates the CARRIAGE, and three pneumatic valves (L) which are connected to the pneumatic cylinders on the FRAME (I) and CARRIAGE (F) by high pressure air hoses (J). On the bottom part of the frame are attached two 30 cm vertical brass guide rails for the CARRIAGE to slide on (See Fig. S-4c).

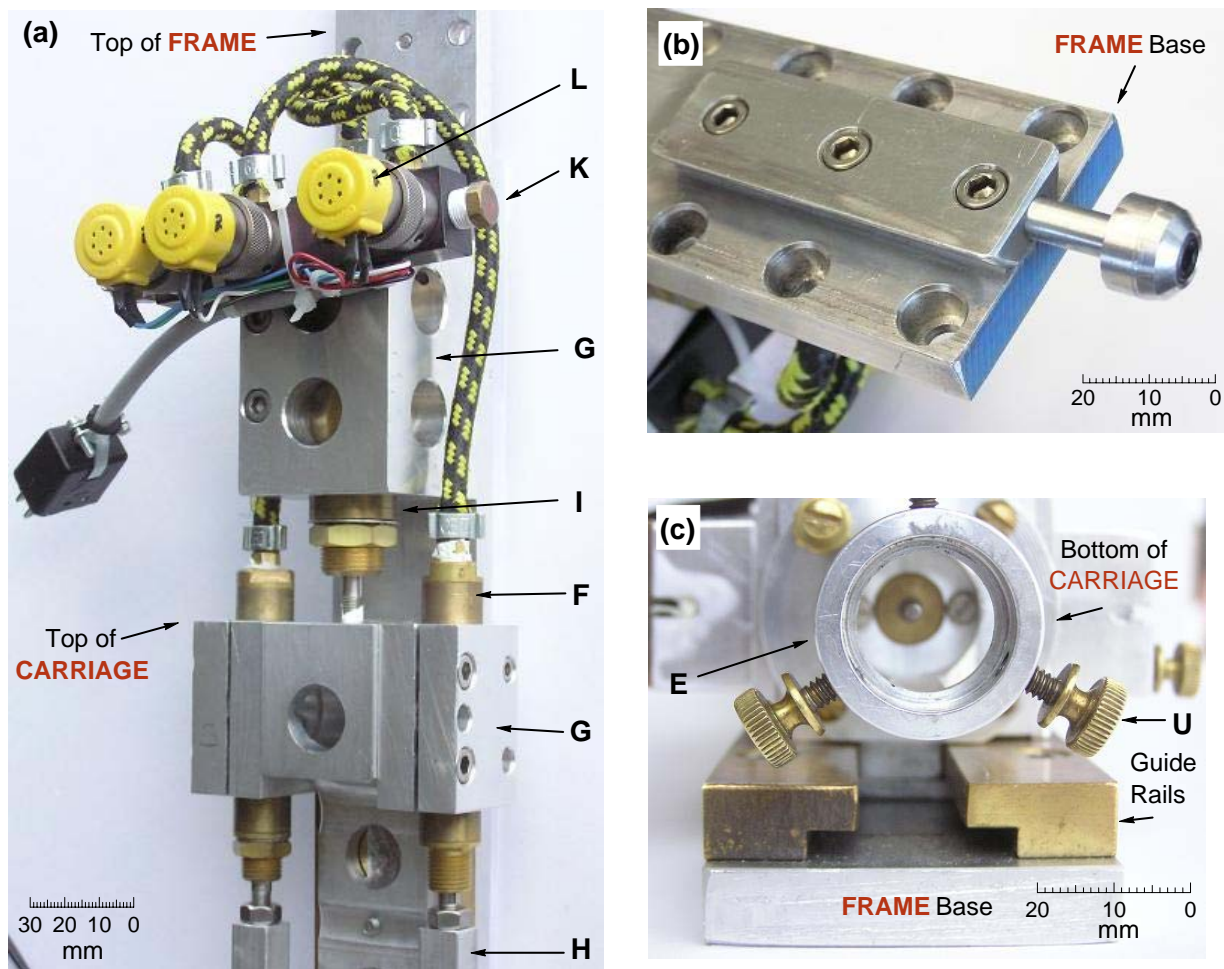


Figure S-4. Photographs of portions of the injector. (a) Top of the FRAME and CARRIAGE, showing the electronic valves and pneumatic cylinders. (b) The mounting bracket on the back of the FRAME at the top end. (c) The bottom of the FRAME and CARRIAGE, showing guide rails, and the mount for the INSERT.

The CARRIAGE consists of a 30 x 3.8 x 3.8 cm aluminum base, extensively machined and drilled to reduce weight, improve visibility, and provide points of attachment for mounting the working parts. The CARRIAGE slides on the brass rails of the FRAME (see Fig. S-4c), and has a 2.5 cm range of up-down motion. Mounted on the side of the CARRIAGE are two aluminum housings (C), designed to hold 1 mL Hamilton gas-tight syringes (Fig. S-5a). The housings can be changed to accommodate other syringe sizes. Recessed into the bottom end of the CARRIAGE is a 12 volt DC electric motor (D) capable of operating at 15,200 rpm (no load) (Radio Shack High-Speed 12VDC, 2.5 cm x 1.3 cm diameter). Bolted to the CARRIAGE below the stirrer is an adapter (E) which provides for attachment of the INSERT (see Figs. S-4c and S-5a). The syringes are actuated by spring-return pneumatic cylinders (F) with 2.5 cm strokes operating at a pressure of 100 psi (Clippard 9/16" (1.4 cm) Bore, Brass Heavy Duty Minimatic Cylinder with Single Acting Spring Return and Stud mount, H9S-1S), which are attached to the sides of the CARRIAGE by aluminum clamps (G). The cylinder pistons are connected to adjustable aluminum plungers (H). The CARRIAGE is moved on the guide rails by a third spring-return pneumatic cylinder (I), which is attached to the FRAME by an aluminum clamp (G). The pneumatic cylinders are connected with high pressure tubing (J) to a manifold (K). The manifold is controlled by a series of electronic valves (Clippard ET-3M-6VDC) (L), which are connected to and actuated by the CONTROLLER.

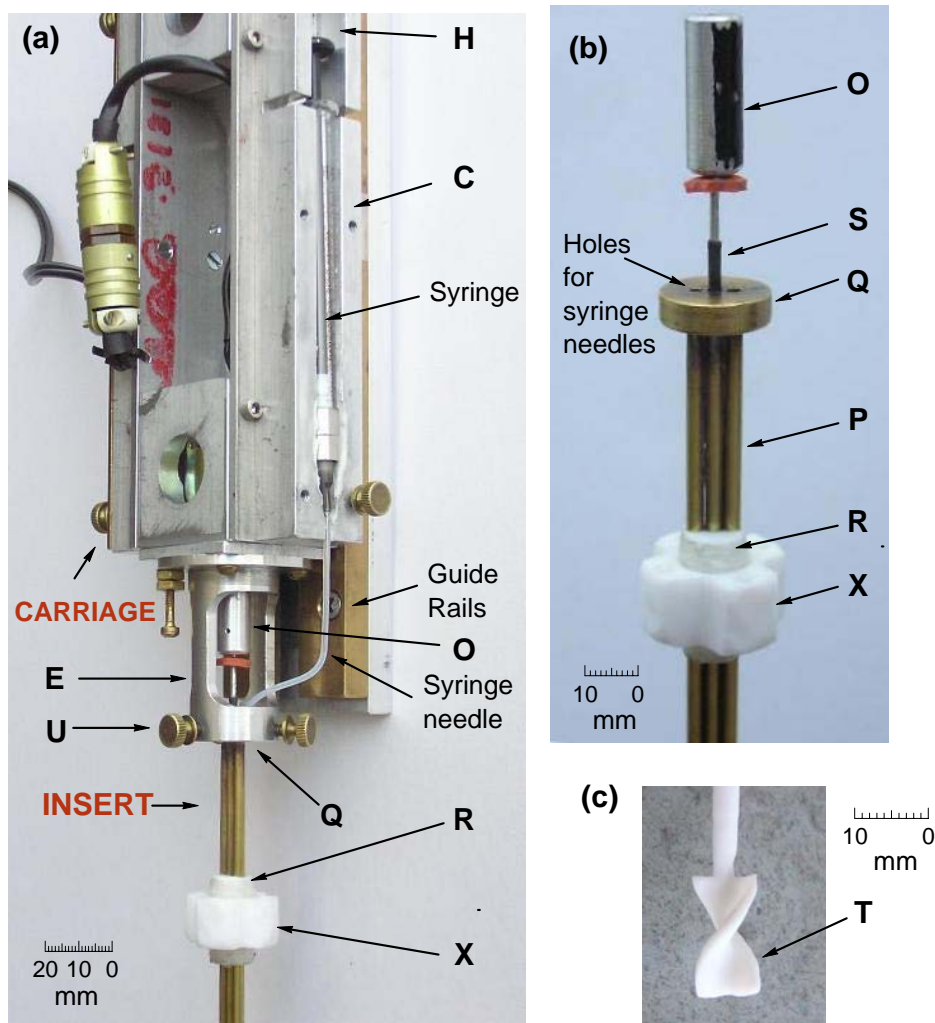


Figure S-5. Photographs showing details of the CARRIAGE and INSERT. (a) The bottom part of the injector, with one syringe and the INSERT mounted on the CARRIAGE. The safety cover (B) which normally encloses the syringe housing (C) has been removed. (b) Details of the top of the INSERT, set up for use without the SCAFFOLD (the Teflon spacers X would be removed if the SCAFFOLD were being used). (c) The Teflon stirrer paddle.

The INSERT (Fig. S-5b) is placed directly into the probe (spacers **X** attached to INSERT), or into the SCAFFOLD, if it is in use (spacers **X** attached to SCAFFOLD). The INSERT consists of three pieces of 0.32 cm (1/8") OD brass tubing (**P**) soft welded into a 2.5 cm diameter brass cylinder (**Q**). The outer tubes, which hold the syringe needles, are 84 cm long, designed to reach to just above the top of the NMR tube, since there is not enough space to fit these into the tube. The middle tube (which holds the stirrer shaft) is 92 cm long, designed to reach well within the NMR tube. The three brass tubes are held in place with Teflon guides (**R**) to give them additional strength and to center them in the SCAFFOLD. A 1.6 mm (1/16") x 91 cm aluminum stirrer shaft (**S**), with an aluminum shaft coupling (**O**) attached to the top, is inserted into the center brass tube. The coupling has a vertical black stripe to allow measurement of the stirring rate using a tachometer. A hand crafted two bladed Teflon paddle (**T**) is attached to the bottom end of the shaft. The one shown in Fig. S-5c was the most effective of several designs tried. Upon assembly, the shaft coupling (**O**) is connected to the electric stirrer motor and the brass cylinder (**Q**) is placed inside the internal guide connector (**E**), and fastened with thumb screws (**U**). The bottom of the stirrer paddle should be just above the sample level in the NMR tube, and the injection needle should end just above the top of the stirrer paddle.

The SCAFFOLD is an optional insert into the spectrometer bore which protects the top of the spectrometer, and provides a support for the INSERT during assembly of the apparatus. It consists of a 82 cm long piece of 1.0 cm (3/8") ID brass tubing (**V**), which has been soft welded to a 1 cm thick brass plate (**W**). The 13 x 7.6 cm brass plate has the safety benefit of protecting the bore from any potential falling parts. The brass tube is fitted with Teflon spacers (**X**) which center the brass tube in the probe, and which can be easily exchanged to fit different sized bores. The spacers have cutouts to allow the cooling and spinner gas to pass. A perforated 1.3 cm thick Teflon disk (**Y**), which rests directly on the room temperature shim stack, is used to allow spinner air to escape from under the scaffold. For extremely air sensitive samples an additional flow of argon down the top of the spectrometer bore is used. To allow room for the Tygon hose which connects to an Argon cylinder, the SCAFFOLD is not used, and Teflon spacers (**X**) are placed on the Teflon guides (**R**) of the INSERT to align it for proper insertion into the NMR probe (as shown in Fig. S-4b).

The CONTROLLER operates in either manual or pulse-program control. For manual control a set of 4 switches are used to lower and raise the CARRIAGE, start and stop the stirring motor, and perform the injections of the two independently controlled syringes. The timing and duration of these operations can also be controlled by the spectrometer, using parameters written into the pulse program (see below), and this is the normal mode of operation.

Temperature Control. Our RINMR kinetic studies benefitted greatly from the ability to measure the actual internal temperature of the sample before, during and after an injection using our internal ^{13}C chemical shift thermometer (Me_3Si) $_3\text{CH}$,^[S-9] which shows an almost linear temperature dependence of the chemical shift (ca 1 Hz per degree) between the SiCH_3 and the CH carbons. We normally use ca 2-4 μL of 10% ^{13}C enriched material in all samples for measurement of temperature before and after an injection. If a larger amount (ca 20 μL) is used, then the ^{13}C signals can be seen in one scan, and the temperature of the sample can be measured during an actual injection on a seconds time scale. Fig. S-6 shows the results of such experiments. There is a 4-5 degree jump in temperature during a typical injection of 0.2 mL of substrate into 4 mL of a cold (< -100 °C) solution. The temperature returns to the pre-injection value in under 2 min. Since this is often a key time period for experiments, we developed a procedure to maintain a constant temperature by raising the console temperature setting an appropriate amount (5 degrees) ca 10 s before the injection (Fig. S-6c).

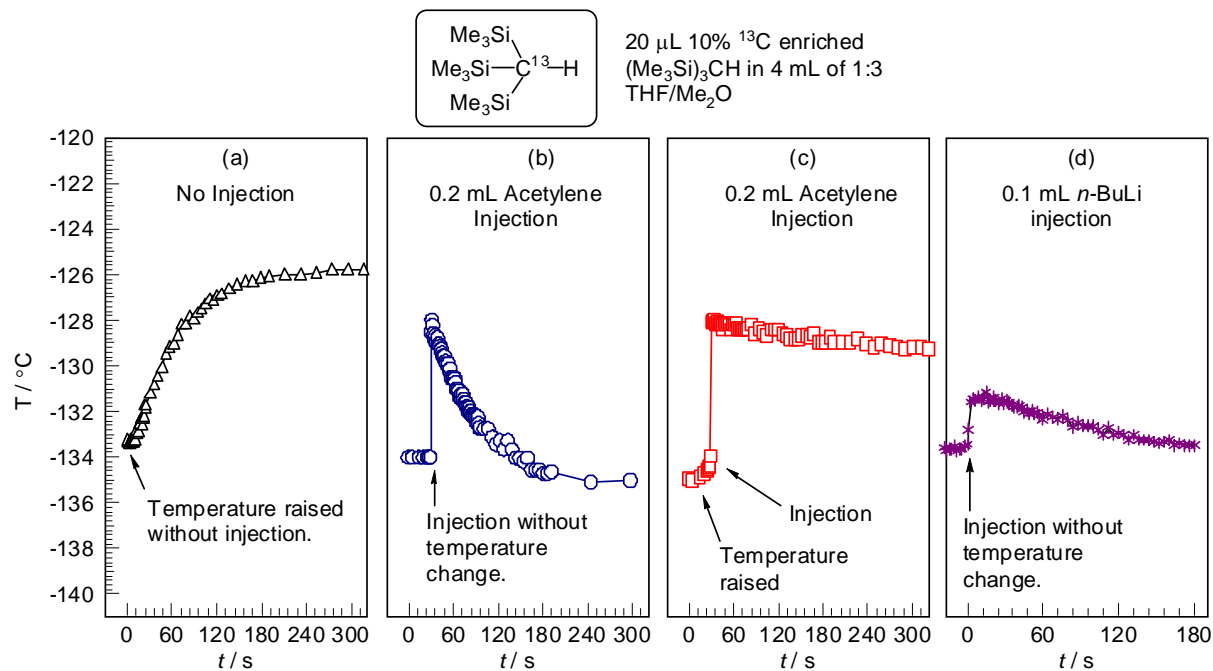


Figure S-6. Sample temperature changes during RINMR experiments. (a) Response of sample temperature to a 5° increase in spectrometer temperature setting. (b) Injection of a 0.2 mL sample of (trimethylsilyl)acetylene. (c) Spectrometer temperature setting raised 5° 10 s before injection of 0.2 mL of (trimethylsilyl)acetylene. This is the procedure used for most of the RINMR experiments reported. (d) Injection of 0.1 mL of a 2.5 M solution *n*-BuLi in hexanes. Note that the injected volume is one-half that of the other experiments, and temperature jump is also half as large, indicating insignificant heating due to solvation of the *n*-BuLi.

Volume Accuracy of Injection. A weak feature of our experiment is that the volume of injected material cannot be controlled with great precision, nor can multiple small increments of sample be injected because of the ca 146 cm long injection needles, and the on-off nature of our injection method. Whenever possible we checked the amount of reactant injected by NMR spectroscopic analysis of the sample during or after the experiment.

Normal/Inverse Mode of Injection. “Normal” addition (substrate injected into a solution of the lithium reagent) is the most convenient experiment to perform with our apparatus, because it avoids handling of a syringe filled with reactive or air-sensitive material (for example, the ca 146 cm needle has to be threaded into the INSERT with the syringe filled with substrate). Most of the experiments reported in this paper used normal addition. Successful inverse-mode additions were also carried out. For example, Fig. S-7 shows a RINMR experiment where *n*-BuLi in hexane was injected into 3:1 $\text{Me}_2\text{O}/\text{THF}$ at -131°C (a similar experiment was reported by McGarrity and coworkers^[S-1b] at -84°C in pure THF). Initially the *n*-BuLi is present as only the tetramer and the dimer grows in over the course of 1 h.

This experiment also demonstrates that the heat of solvation of the *n*-BuLi and that carried into the cold sample by the injected warm solution is dissipated rapidly since only traces of *n*-BuLi dimer are initially formed. The results of an experiment where an *n*-BuLi solution in hexanes was injected (Fig. 6d) show that heat of solvation of the injected lithium reagent by THF and Me_2O is not significant, since the temperature increase was very similar to that seen when the same volume of solvent alone was injected.

The inverse mode of injection is particularly useful for studying the reactivity of *n*-BuLi tetramer, since it produces an initial nonequilibrium state that is $>95\%$ tetramer. This mode was used for the experiments of Fig. S-17 and S-18 (reaction of *n*-BuLi with phenylthioacetylene and *p*-fluorobenzaldehyde).

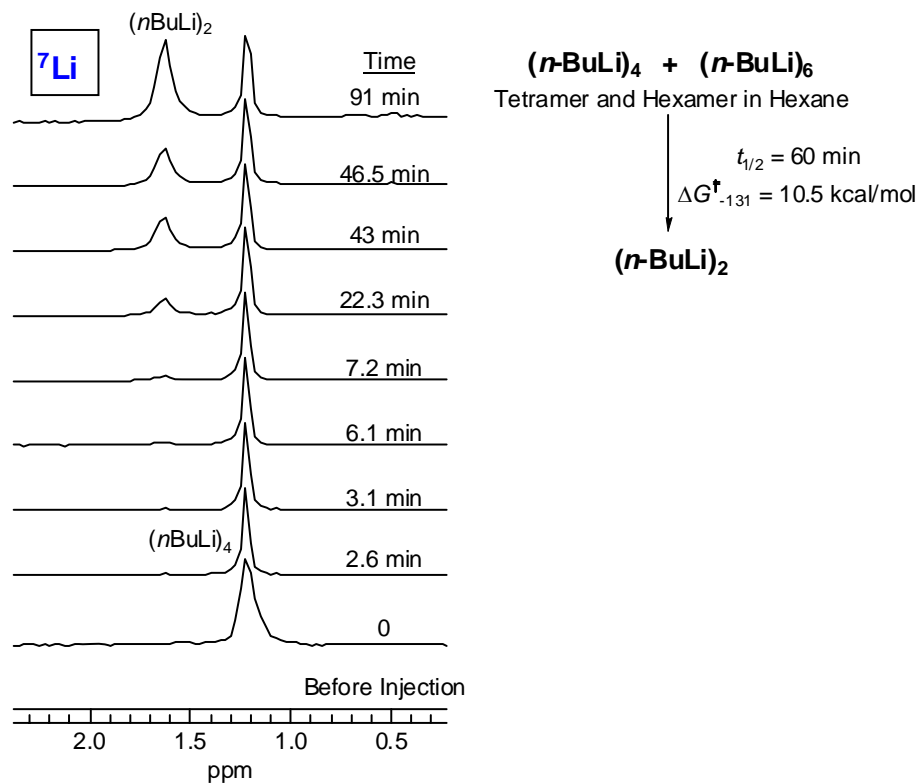


Figure S-7. An inverse mode injection of 0.05 mL of $n\text{-BuLi}$ (2.6 M in hexanes) into 4 mL of 1:3 THF/Me₂O at $-131\text{ }^\circ\text{C}$.

Low Temperature Experiments. The lower temperature limit of our experiments was dictated by crystallization of solvent and solubility of substrate. We were interested in measuring the properties of lithium reagents in solvents in which they are typically used (most often THF or other ethers). The 1:3 THF/Me₂O solvent mixture chosen after considerable experimentation is a compromise between maintaining THF-like solvent polarity and allowing work routinely down to $-135\text{ }^\circ\text{C}$ without crystallization of THF. If solvent mixtures richer in THF are used, crystallization *during the injection and when the sample is stirred* becomes a serious problem. Note that such samples can often be used at considerably lower temperatures for extended periods of time with no solvent crystallization if the sample is undisturbed. We conclude that many of the NMR experiments we and others have carried out in THF-ether and THF-dimethyl ether mixtures at temperatures near and below $-130\text{ }^\circ\text{C}$ were supersaturated in solvent, and probably also frequently in substrate. The material to be injected was added neat, or dissolved in THF-ether mixtures, since solvents containing Me₂O (b.p. $-23\text{ }^\circ\text{C}$) could not be used.

Saturation. Most of the experiments reported here used ^7Li NMR spectroscopy ($I = 3/2$) to monitor the progress of the reaction. We were able to achieve satisfactory signal-to-noise in a single transient. Repetition rates as fast as 0.25 seconds could be used with only minor saturation of the tetramer signal (see pre-scans in Fig. S-8) ($T_{1(\text{Tetramer})} \leq 0.11\text{ sec}$, $T_{1(\text{Dimer})} \leq 0.03\text{ sec}$). In experiments in other contexts, use of ^1H and ^{19}F NMR spectroscopy required repetition rates of $\geq 2\text{ s}$, and with ^{13}C (enriched), $\geq 3\text{ s}$.

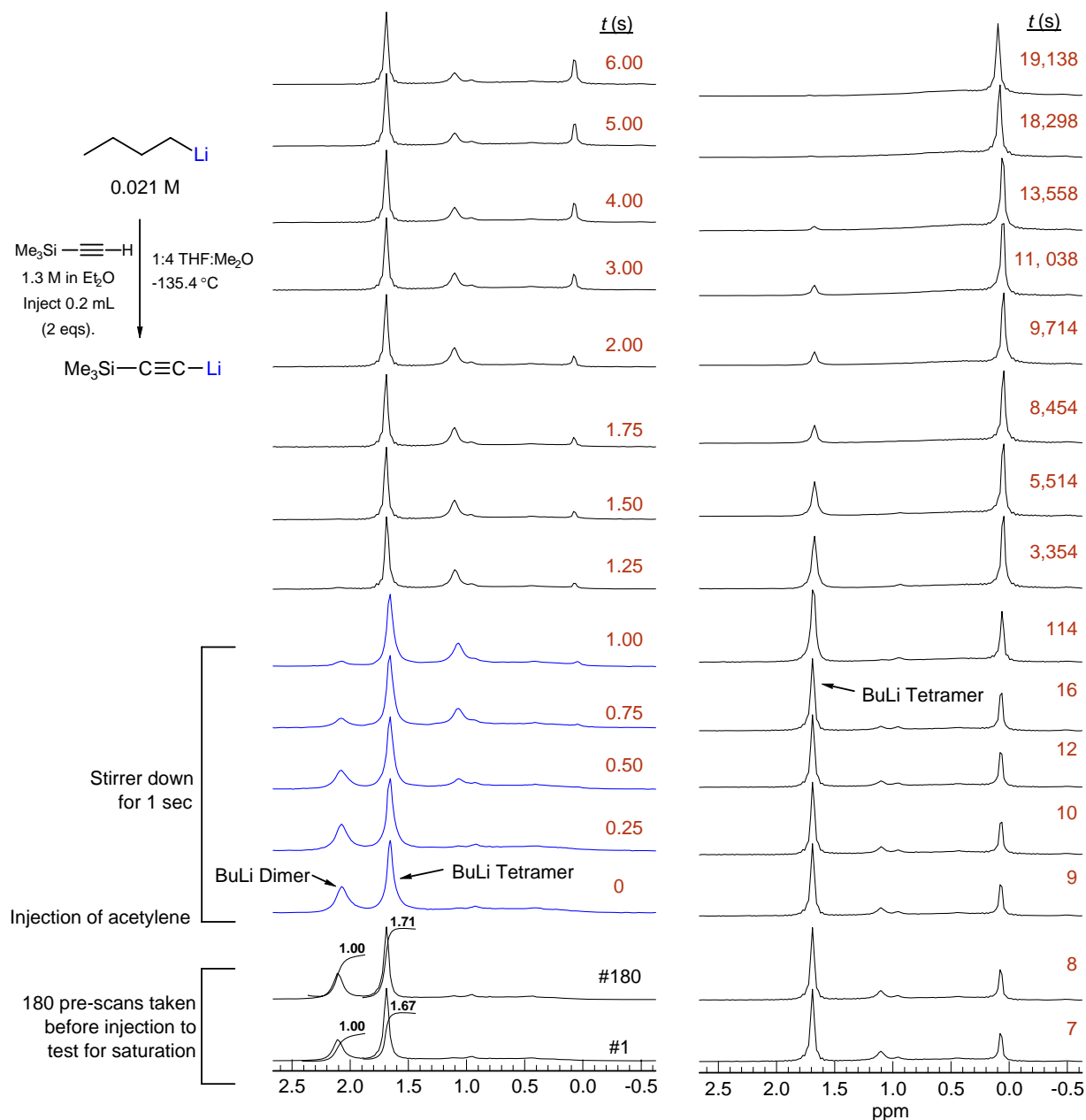


Figure S-8. Sample RINMR experiment of the reaction of *n*-BuLi with (trimethylsilyl)acetylene. Spectra were taken every 0.25 s for 45 s (180 spectra) then every 60 s for 20,000 s. The ^7Li NMR spectra with the Teflon stirrer in the sample ($t = 0\text{--}1$ s, blue spectra) are only marginally broader than after the stirrer was raised ($t > 1$ s).

Accuracy of Timing. Several kinds of experiments showed that complete mixing of injected material in THF- Me_2O mixtures at -130°C with the stirrer motor spinning at 4,000 to 6,000 rpm required ca 1 s (this includes lowering the CARRIAGE, injecting, stirring for 0.6 s and raising the CARRIAGE). There is thus an inherent inaccuracy of ± 0.5 s in the time measurement. To get reasonably accurate rate constants ($\pm 15\%$) we need a half-life of at least 15 s ($\Delta G^\ddagger > 9$ kcal/mole), although poorer quality data can be obtained between 3-15 s.

Air/water Problem. The RINMR experiment with our apparatus is inherently an open-tube operation, although the opening of the NMR tube is partially blocked by the stirrer and injector needle assembly. With air-sensitive substrates the spectrometer must be operated using pure dry nitrogen for the cooling gas stream as well as for activating the sample spinner so that the spectrometer bore is an anaerobic environment. Nevertheless, we found that small amounts of air occasionally get into the sample (we showed that addition

of 6 mL of air into a 0.08 M sample of *n*-BuLi resulted in complete destruction of *n*-BuLi within 30 min). An argon flush (1 cm diameter Tygon tube inserted 12 cm into the magnet bore running 36 mL/sec) maintained throughout the experiment and especially during assembly of the apparatus, improved reproducibility in experiments with *n*-BuLi. In this way, we could reliably work with *n*-BuLi in an open tube even in experiments lasting up to 10 h. This precaution did not seem to be needed for less reactive lithium reagents, for example lithium (trimethylsilyl)acetylide.

General Procedure for a RINMR Experiment. Septum-sealed samples are prepared in a 10 mm NMR tube sawed to a length of 18 cm (see experimental for details of sample preparation). The material to be injected (when not *n*-BuLi) is weighed into a separate, septum-sealed, N₂ purged flask and dissolved in THF/Et₂O at a concentration appropriate for a 0.2 mL injection. The NMR sample (still sealed with a septum) is inserted into the probe, and preliminary spectra are collected to adjust spectrometer tuning, check the quality and concentration of the sample using ⁷Li and ¹H NMR spectroscopy, and measure the temperature of the sample using ¹³C NMR.^[S-9]

The sample is then raised, the septum is removed, and the open NMR tube is lowered into the spectrometer with great care to minimize exposure to air. Argon purging is started and the apparatus is assembled as follows: the Teflon stirrer is attached to the stirrer shaft of the INSERT, which is placed carefully in the probe and into the NMR tube. The INJECTOR assembly is attached to the ceiling bracket, the brass ring (Q) of the INSERT is attached to the guide connector (E), and the motor coupling is attached to the motor. The air supply is attached to the pressurized air inlet (M) and the CONTROLLER is connected to the injector relays. At this point the spectrometer temperature is stabilized to ca 5° lower than the target temperature for the experiment.

The actual injection is performed as follows. The pulse program is started, which includes a number of user-defined pre-injection scans (the exact number depends on the acquisition time) set to last about 20 s. Approximately 10 s prior to the injection the spectrometer temperature setting is raised ca 5 °C (the offset has to be empirically determined as depicted in Fig. S-6). After the pre-injection scans the automated pulse program lowers the CARRIAGE, starts the stirrer and injects the sample, continues stirring for 0.6 s, stops the stirrer, raises the CARRIAGE and continues collecting spectra. Depending on the length of the experiment, spectra are typically taken at 0.8 s intervals for a few minutes (although intervals as short as 0.25 s work well for ⁷Li), a period termed “fast acquisition” (see below). A longer time interval (15-60 s) is selected for the remainder of the experiment, a period termed “slow acquisition.” At the completion of the experiment, the temperature of the sample is again checked,^[S-9] and post-kinetics analyses of the sample are performed (e.g. ¹H NMR for concentration determination and ¹³C NMR for product determination).

Spectrometer Control of the Injector. The Bruker Timing Control Unit’s extra output lines are used to control the actions of the injection apparatus. These lines are available to the user through the BP1 connector on the back of the console. These are TTL lines that are normally in the high state, at 5 volts. They are controlled by changing the bits in a register through pulse programming. The specific register that controls the outputs of connector BP1 is NMR Word 4. The specific lines that are available to the user are controlled by bits 3, 4, 6 and 7 (Table S-1). They correspond to pins Z, DD, S and W respectively on connector BP1. These output lines are cabled to a control box. This box uses these digital inputs to switch electrical lines that control three valves and one motor, as follows. The control box contains the switching circuitry and a power supply for the motor and valves. There are also manual override switches for each of the valves and a motor speed control dial, as well as a motor voltage meter.

Table S-1. Electronic controller box configuration.

NMR Word Bit #4 Bit #	Connector BP1 Pin#	Controller Box Configuration
3	Z	Valve #1 (Raise/Lower CARRIAGE)
4	DD	Valve #2 (Activate Injection Plunger 1)
6	S	Valve #3 (Activate Injection Plunger 2)
7	W	Stirrer Motor on/off

Pulse Program for Proton or Lithium Kinetics Runs. The Bruker Avance-360 spectrometer utilizes XwinNMR acquisition and processing software. We use a 2D pulse program (shown below) to control the injection and spectral acquisitions. The program can be written to contain as many loops as needed with specific delays for each loop. The first pre-injection loop (10-20 s) allows us to monitor the sample prior to the injection, check for signal saturation, and provide the time needed to change the temperature setting. During the injection loop starting at line 2 and occurring only once, the timing is as follows. Following d5, and d1, acquisition of a single scan occurs. Following completion of the acquisition time, the CARRIAGE is dropped followed by a delay of d11 (typically 0.5 s). Delays of zero are not allowed, so in order to stir at essentially the same time as the injection, d14 must be set to a small finite value (e.g. 1 ms). After the injection, stirring is continued for a delay of d13. This is typically kept short (0.5 s), after which the apparatus is raised again. For the stirring motor to be shut off at the same time the apparatus is raised, d21 is set to 1 ms. If d21 is set slightly longer (such as 0.5 s), the motor will continue stirring *while* the apparatus is raised. Both methods lead to efficient mixing. With delay d24 also small (1 ms), acquisitions continue (line 4) immediately following the completion of the injection and stirring procedure. The command 'go = #' comes into effect when the number of scans (NS) per spectrum is greater than 1, where NS is an external acquisition parameter. In such a case, 'd1' and 'p1' are repeated. Thus 'd1' is a repeated relaxation delay to prevent saturation from multiple scans, whereas 'd5' and 'd6' represent the delay between experiments, and thus determine how frequently kinetic data points are collected.

"l3 = td1 - l0 -l1 -l2"

"d19 = 30 m"

```
ze
d5
1  d1
   p1*0.33 ph1
   go=1 ph31 ;data acquisition, cycle back to line 1 if #scans >1
   d19 wr #0 if 0#zd ;d19 is delay for disk I/O
   lo to 1 times l0 ;loopcounter 0, pre-injection loop, l0 repetitions

2  d5
3  d1
   p1*0.33 ph1
   go=3 ph31
   d19 wr #0 zd
   lo to 2 times l1 ;loopcounter 1 injection loop (l1 = 1 for a single cycle)

   d11 setnmr4|3 ;valve 1 - turn on drop
   d14 setnmr4|7 ;valve 4 - turn on stirrer motor
   d13 setnmr4|6 ;valve 3 - turn on inject
   d21 setnmr4^3 ;valve 1 - turn off drop
   d24 setnmr4^7 ;valve 4 - turn off stirrer motor

4  d5
5  d1
   p1*0.33 ph1
   go=5 ph31
   d19 wr #0 if 0# zd
   lo to 4 times l2 ;loopcounter 2, fast acquisition loop, l2 repetitions

6  d6
7  d1
   p1*0.33 ph1
   go=7 ph31
   d19 wr#0 if #0 zd
   lo to 6 times l3 ;loopcounter 3, slow acquisition loop, l3 repetitions

   d23 setnmr4^6 ;valve 3 - turn off inject

exit

ph1= 0 2 2 0 1 3 3 1
ph31= 0 2 2 0 1 3 3 1
```

The command **ased** opens a dialog box in which to set the acquisition parameters for the experiment (Table S-2).

Table S-2. The acquisition parameter list in XwinNMR from the command **ased**.

ASED - acquisition parameters

PULPROG	kinauto		pulse program for acquisition
td	1333 ^[a]		time domain size
ns	1		number of scans
ds	0		number of dummy scans
swh	1666.7 ^[a]		sweep width in Hz
aq	0.8 ^[a]	sec	acquisition time (typically 0.8 - 2 s)
rg	1200 ^[a]		receiver gain
dw	104.8 ^[a]	usec	dwel time
de	6 ^[a]	usec	pre-scan delay
d1	0 ^[a]	sec	relaxation delay
d5	0 ^[a]	sec	interexperiment delay fast acquisition
d6	60 ^[a]	sec	interexperiment delay slow acquisition (15-120 sec)
d11	0.6	sec	delay following apparatus drop
d13	0.5	sec	delay following injection
d14	0.001	sec	delay following start of motor
d19	0.03 ^[b]	sec	d19 = 30 ms (delay for disc I/O)
d21	0.001	sec	delay following apparatus raise (0.5 sec works also)
d23	0.001	sec	delay following injection OFF
d24	0.001	sec	delay following motor STOP
i0	15		pre-injection scans (typically 9-15)
i1	1		loopcounter during injection (typically 1)
i2	200 ^[a]	sec	loopcounter fast acquisition (depends on reaction rate)
i3	211 ^[b]	sec	loopcounter slow acquisition (depends on reaction rate)

[a] These parameters (in red) vary from experiment to experiment and depend upon the nucleus observed and the time scale of the reaction. [b] The values in **bold** cannot be altered using this dialogue box.

An additional parameter, not available on the **ased** parameter list is **td1**. It is the number of increments along the time axis. The number of the distinct spectra in loop 0 (the pre-injection scans), loop 1 (the injection scan), loop 2 (fast acquisition) and loop3 (slow acquisition) add up to **td1**, which is user defined. The parameter **i3** is automatically calculated ($i3 = td1 - i0 - i1 - i2$). The complete acquisition parameter listing is accessed with the command **eda** and is used to set **td1**.

That data are saved as a 2-dimensional SER file. Individual FIDs are extracted in XwinNMR from the

2D file to their own experiment number using the command RSER. Specifically, the command "**rsr 20 620**" extracts the 20th spectrum and places it into experiment number 620. The individual FIDs are then worked up in NUTS like normal 1D spectra. Peak areas are determined using the NUTS line fitting routine.

S2. General Experimental.

Tetrahydrofuran (THF) and Et₂O were freshly distilled from sodium benzophenone ketyl before use. Me₂O was dried with *n*-BuLi directly prior to use in a graduated conical cylinder and distilled via cannula into the NMR tube. Glassware was placed overnight in an oven at 110 °C or flame-dried before purging with N₂ to remove moisture. NMR tubes, injection needles and syringes were kept dry by storing them under low pressure in a glove box antechamber. Common lithium reagents were titrated using *n*-propanol in THF with 1,10-phenanthroline as indicator.^[8-10] Temperatures of -78 °C were achieved with a dry ice/acetone bath and -20 °C with a chemical freezer. Kugelrohr distillation temperatures refer to the pot temperature.

Commercially available starting materials and reagents (obtained from Aldrich Chemical Company unless otherwise noted) include: *n*-BuLi (2.5 M in hexane), MeLi (1.4 M in ether), (trimethylsilyl)acetylene (**1a**) (GFS Chemicals), (triphenylsilyl)acetylene (**1b**), (*p*-tolylsulfonyl)acetylene (**1d**), 3-methoxybenzyl alcohol, Me₃SnCl.

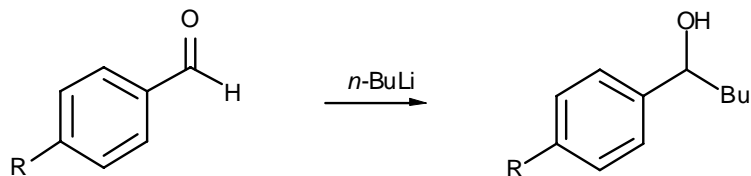
Low-temperature heteronuclear NMR experiments were performed on a 360 MHz spectrometer with a 10 mm broadband probe at the following frequencies: 90.556 MHz (¹³C), 139.905 MHz (⁷Li). Spectra were obtained in undeuterated ether solvents with the spectrometer unlocked. ¹³C spectra were acquired with composite pulse decoupling (CPD) and referenced internally to the C-2 carbon of THF (68.0 ppm). Lorentzian multiplication (LB) was applied to ¹³C spectra. ⁷Li and ⁶Li spectra were referenced externally to 0.3M LiCl/MeOH standard (0.00 ppm). Samples were prepared in thin-walled 10 mm NMR tubes, fitted with 9 mm septa, wrapped with parafilm and purged with N₂ (or Argon for RINMR experiments). Samples were prepared and stored at -78 °C.

S3. Syntheses

deutero-(Trimethylsilyl)acetylene (*d*-1a). To a 100 mL RB Schlenk flask equipped with a stir bar and purged with N₂ was added (trimethylsilyl)acetylene (8.0 mL, 56.6 mmol) and 50 mL of Et₂O. The stirring solution was cooled to -78 °C and *n*-BuLi (2.5 M in pentane, 20 mL, 50 mmol) was added. After 20 min the solution was allowed to warm to room temperature. A high vacuum pump was connected to the Schlenk line to evaporate all solvents and dry the resulting white solid. After 1 h the flask was taken off vacuum and backfilled with N₂. D₂O (0.9 mL, 50 mmol) was added *very slowly* as the reaction is highly exothermic and vaporizes the acetylene if done too quickly. The white slurry was stirred vigorously for 15 min. The septum was removed and the flask equipped with a 3-way distillation adapter connected to a 25 mL conical collecting flask (with the thermometer joint closed with a glass stopper). The Schlenk line was connected to the vacuum pump but kept closed to prepare for distillation. The slurry was frozen by submerging the flask in N₂(l) for 5 min and the Schlenk line was opened to evacuate the system. After 5 min the flask and setup were raised and rotated to submerge the collecting flask. As the flask containing acetylene and LiOH warmed the acetylene condensed in the collecting flask. A clear liquid (4.82 g, 97%) was collected that contained by NMR ≤0.6 % of the proteo-acetylene and a small amount (≤ 2 mol%) of ether. ¹H NMR (300 MHz, CDCl₃): δ 2.4 (s, 0.006 H), 0.2 (s, 9.0 H). ¹³C NMR (90 MHz, THF): δ -0.17 (s), 89.2 (1:1:1 t, ²J_{D-C} = 6.5 Hz), 94.7 (1:1:1 t, ¹J_{D-C} = 36.4 Hz).

(Trimethylsilyl)phenylthioacetylene. This compound was synthesized according to a literature procedure.^[S-11] Purification by kugelrohr distillation (0.02 torr, 125-135 °C) gave an 88% yield of a pale yellow oil. ¹H NMR (300 MHz, CDCl₃): δ 0.26 (s, 9H), 7.2-7.27 (m, 1H), δ 7.32 - 7.5 (m, 4H).

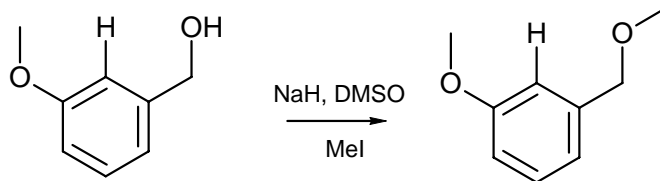
(Phenylthio)acetylene (1c). This compound was synthesized according to a slight modification of a literature procedure.^[S-11] (Trimethylsilyl)(phenylthio)acetylene (3.2 g, 15.5 mmol) was dissolved in 20 mL of CH₃OH and stirred in an open 50 mL RB flask. KF (1.8 g, 31 mmol) was added in addition to 5 drops of H₂O. The clear solution was stirred at room temperature for 80 min, by which time it had turned a pale yellow. The reaction was quenched with aqueous NH₄Cl (10 mL) and extracted with ether (35 mL). The organic layer was washed with water (10 mL). The aqueous layer was extracted sequentially with additional ether (2x20 mL). The organic layers were combined, dried with MgSO₄ and concentrated to give a pale yellow oil (1.56 g, 11.6 mmol, 75%). Over time, the substance turned brown and was typically stored in a -78 °C freezer, where decomposition was kept at a minimum over a period of a few months. Typically before use, the compound was dissolved in hexanes and run through a pipette containing silica gel and MgSO₄. ¹H NMR (300 MHz, CDCl₃): δ 3.26 (s, 1H), 7.21-7.27 (m, 1H), 7.32 - 7.39 (m, 2H), 7.43 - 7.48 (m, 2H). ¹³C NMR (90 MHz, CDCl₃): δ 71.3 (S-C≡C-H), 87.1 (S-C≡C-H), 126.9, 127.1, 129.6, 131.8. MS(EI): M+• = 134.0190 (calcd for C₈H₆S = 134.0196).



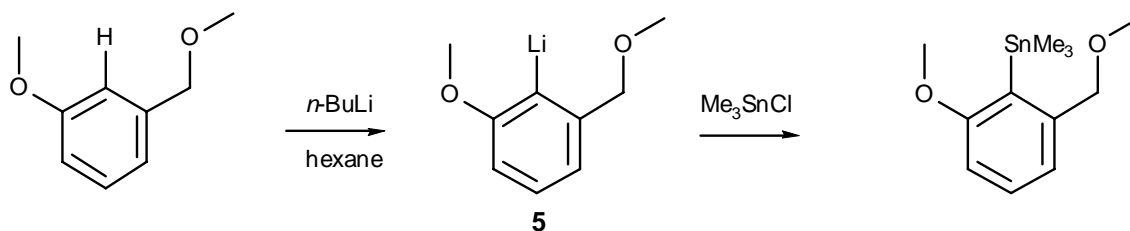
Reaction of *n*-BuLi with Aldehydes. The benzyl alcohol products were prepared separately to confirm the products of the kinetics reactions with benzaldehyde. The aldehyde (5.0 mmol) was weighed into a dry 100 mL round bottom flask equipped with a stir bar. The flask was sealed with a septum and purged with N₂. THF (30 mL) was added and the solution was cooled to -78 °C. *n*-BuLi (2.2 mL, 2.5 M hexanes, 5.5 mmol) was added and allowed to react for 10 min. The solution was then warmed to room temperature and quenched with NH₄Cl (10 mL). The solution was extracted with ether (30 mL) and washed with H₂O (2 x 10 mL) then brine (1 x 20 mL). The organic layer was then run through a short column of MgSO₄ and silica gel. The organic layer was concentrated under low pressure and dried in vacuo (ca 0.1 torr). Quantitative yields were obtained.

1-Phenyl-1-pentanol. This compound has been characterized previously.^[S-12] ¹H NMR (300 MHz, CDCl₃): δ 0.9 (t, *J* = 7 Hz, 3H), 1.3 (m, 4H), 1.8 (m, 2H), 3.1 (br, 1H), 4.7 (dd, *J* = 5.9, 7.6 Hz, 1H), 7.2-7.3 (m, 5H).

1-(4-Diethylaminophenyl)-1-pentanol. ¹H NMR (300 MHz, CDCl₃): δ 0.88 (t, *J* = 7 Hz, 3H), 1.15 (t, *J* = 7 Hz, 6H), 1.2 - 1.45 (m, 4H), 1.6 - 1.85 (m, 3H), 3.33 (q, *J* = 7 Hz, 4H), 4.5 (dd, *J* = 7, 2.4 Hz, 1H), 6.5 (d, *J* = 8.9 Hz, 2H), 7.18 (d, *J* = 8.9 Hz). ¹³C NMR (75 MHz, CDCl₃): δ 12.8, 14.3, 22.9, 28.5, 38.5, 44.6, 74.7, 111.9, 127.4, 131.8, 147.7. MS(ESI): [M+H]⁺ = 236.2021 (calcd for C₁₅H₂₅NO = 236.2014).



3-Methoxymethylanisole. 3-Methoxybenzyl alcohol (4.5 mL, 36 mmol) was added to a stirring slurry of NaH (2.92 g, 60% dispersion, 73 mmol) in 75 mL of DMSO in a 250 mL round bottom flask. After 1 h, MeI (4.5 mL, 73 mmol) was added and allowed to react for 1 h. The reaction was quenched with 50 mL of H₂O, extracted with 3 x 50 mL of 1:1 ether/hexanes. The organic layer was washed with 25 mL of H₂O, 25 mL of brine, dried with MgSO₄ and concentrated to give a faint yellow oil (4.47 g, 86 %). ¹H NMR (300 MHz, CDCl₃): δ 3.40 (s, 3H), 3.83 (s, 3H), 4.45 (s, 2H), 6.85 (m, 1H), 6.93 (m, 2H), 7.27 (t, *J* = 8.1 Hz, 1H). ¹³C NMR (75 MHz, CDCl₃): δ 55.5, 58.4, 74.8, 113.1, 113.6, 120.2, 129.6, 140.1, 160.0.



2-Trimethylstannyl-3-methoxymethyl-anisole. 3-(Methoxymethyl)anisole (0.99 g, 6.54 mmol) and 25 mL of hexane were added to a 50 mL RB flask, purged with N₂, and cooled in an ice water bath. *n*-BuLi (2.35 M in pentane, 0.34 mL, 7.85 mmol) was added and the reaction flask was placed in a 0 °C freezer for 5 days. Trimethyltin chloride (2.4 g, 12 mmol) in 5 mL of THF was added after transferring the reaction flask to an ice water bath. The reaction mixture was extracted with ether, washed with brine, and dried with MgSO₄. After concentrating under low pressure, the resulting yellow oil was purified by Kugelrohr distillation (≤ 150 °C at 0.01 mm Hg) and a clear oil was collected (1.04 g, 3.31 mmol, 51 %). ¹H NMR (300 MHz, CDCl₃): δ 0.50 (s, ²*J*_{1H-119Sn} = 56.3, ²*J*_{1H-117Sn} = 53.8 Hz, 9H), 3.1 (s, 3H), 3.3 (s, 3H), 4.3 (s, ⁴*J*_{1H-Sn} = 4 Hz, 2H), 7.3 (m, 1H), 7.0 (s, 1H), 7.2 (s, 1H). ¹³C NMR (75 MHz, CDCl₃): δ -6.2 (¹*J*_{13C-119sn} = 364 Hz, ¹*J*_{13C-117Sn} = 347 Hz), 55.6, 57.9, 76.2 (³*J*_{13C-Sn} = 23 Hz), 109.2 (*J*_{13C-119sn} = 22 Hz), 121.9 (*J*_{13C-119sn} = 38 Hz), 130.0 (*J*_{13C-119sn} = 6 Hz), 130.2, 146.5, 164.5. [M+H]⁺ = 317.0553 (calcd. for C₁₂H₂₀O₂Sn = 317.0564).

S4. Competition Kinetics

For two reactants (A and B) competing for a deficiency of the same reagent (C) (where both reactions have the same order) the relative rates can be calculated using the formula $k_A/k_B = \ln(X_A \text{ left})/\ln(X_B \text{ left})$. “ $X_A \text{ left}$ ” and “ $X_B \text{ left}$ ” are defined as the mole fractions of the two starting materials remaining at the end of the reaction relative to the amount of starting materials at the beginning of the reaction. In these experiments A and B are two acetylenes, C is *n*-BuLi dimer. Data are summarized in Table 3.

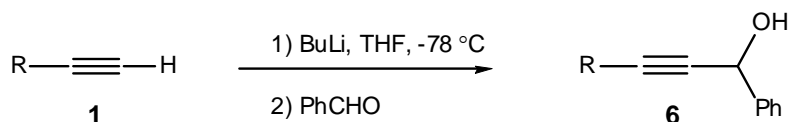
Competition Experiments with *n*-BuLi. A mixture of two acetylenes (0.4 - 2 mmol) (the less reactive acetylene in excess) was prepared as a solution in 4 mL of 1:3 THF/Me₂O, in a 10 mm NMR tube. A deficiency of *n*-BuLi (0.10 mL, 0.25 mmol, 2.5 M hexanes) was added to the sample at -128 °C using the rapid-injection apparatus and allowed to react to completion (ca 2 h) as determined by ⁷Li NMR. After warming to -80 °C, a solution of benzaldehyde (0.1 mL, 0.3 mmol) in THF was injected and allowed to react for 10 min. The sample was removed from the spectrometer and quenched with propionic acid. The mixture was extracted with Et₂O (20 mL), washed with NaHCO₃(aq) (2 x 5 mL), brine (1 x 10 mL) and concentrated. The ratios of products and remaining starting material were determined by ¹H NMR integration with CDCl₃ as solvent (300 MHz), using the propargylic and acetylenic protons, and pentachloroethane as an internal standard.

Competition Experiments with 2-Methoxy-6-(methoxymethyl)phenyllithium (5): A sample of **5** was prepared (see below) and checked by ¹³C and ⁷Li NMR spectroscopy. Using the rapid-injection apparatus a solution of two acetylenes (0.5 - 2 mmol, the less reactive acetylene in excess) dissolved in THF was injected. The temperature for these experiments needed to be -100 °C or higher so that the rate of conversion from the tetramer to the reactive aggregate was fast enough to give convenient reaction times (< 2 h). The method of injecting a solution of the unreactive aggregate in a less polar solvent, as used for *n*-BuLi, was not viable due to the low solubility of the aryllithium in ether. The reaction was followed by ⁷Li NMR spectroscopy to ensure reaction completion. For reactions involving (trimethylsilyl)acetylene, which is lost upon workup, the acetylene concentration was determined *in situ* by ¹H NMR spectroscopy prior to the reaction quench. A solution of benzaldehyde in THF was injected, which reacted within a few minutes. The sample was ejected from the spectrometer, quenched with 3 mL of NH₄Cl(aq) and allowed to warm to room temperature. The product was extracted with 5 mL of ether and the organic layer was dried with MgSO₄ then concentrated under low pressure.

Table S-3. A summary of relative rate constants determined by competition kinetics. The numbers outside of the parentheses are the average of the numbers inside the parentheses.

	H/D	Ph ₃ Si/Me ₃ Si	PhS/Ph ₃ Si	PhS/Me ₃ Si
BuLi	38 (16, 55, 43)	60 (50,70)	57 (66, 47)	3800 (4200, 60x57)
ArLi (5)	66 (75, 56)	46 (47, 26, 65)	75 (51, 99)	2875 (2300, 75x46)

For characterization the benzaldehyde adducts were prepared and purified independently.



R = (a) Me₃Si- (b) Ph₃Si- (c) PhS-

Propargyl Alcohols (6a-c). *n*-BuLi (0.1 mL, 2.5 M/hexanes) was added to a THF (3 mL) solution of an acetylene (0.03 mmol) at -78 °C. After 5 min, benzaldehyde (0.025 mL, 0.25 mmol) was added and allowed to react for 5 min. The reaction was quenched with NH₄Cl(aq) and allowed to warm to room temperature. The product was extracted with 5 mL of ether and the organic layer was dried with MgSO₄, then concentrated under low pressure. Residual benzaldehyde, (phenylthio)acetylene and/or (trimethylsilyl)acetylene were removed under high vacuum (ca 0.2 torr). 1-Phenyl-3-(triphenylsilyl)prop-2-yn-1-ol was purified by column chromatography using silica and 1:9 ethyl acetate/ hexanes eluent.

1-Phenyl-3-(trimethylsilyl)prop-2-yn-1-ol (6a). ^[S-13] ¹H NMR (300 MHz, CDCl₃): δ 0.21 (s, 9H), 2.45 (s, br, 1H), 5.44 (s, br, 1H), 7.3-7.4 (m, 3H), 7.52-7.57(2H). ¹³C NMR (75.5 MHz, CDCl₃): δ 0.045, 65.1, 91.7, 105.2, 127.0, 128.6, 128.8, 140.5. MS(EI): 204.1 (calcd. for C₁₂H₁₆SiO = 204.3433).

1-Phenyl-3-(triphenylsilyl)prop-2-yn-1-ol (6b). ¹H NMR (300 MHz, CDCl₃): δ 2.42 (d, *J* = 6.5 Hz, OH), 5.57 (d, *J* = 6.5 Hz, CH), 7.3-7.5 (m, 12 H), 7.5-7.7 (m, 8H). ¹³C NMR (75 MHz, CDCl₃): δ 65.4, 87.1, 109.9, 127.0, 128.2, 128.7, 128.9, 130.2, 133.3, 135.8, 140.2. MS(EI):M⁺ = 390.1437 (calcd. for C₂₇H₂₂OSi = 390.1440).

1-Phenyl-3-(phenylthio)prop-2-yn-1-ol (6c). ¹H NMR: (300 MHz, CDCl₃): δ 2.7 (s, br, 1H), 5.7 (s, 1H), 7.17-7.25 (m, 1H), 7.27-7.44 (m, 9H), 7.54-7.58 (m, 2H). ¹³C NMR (75.5 MHz, CDCl₃): δ 65.70 (CH), 74.20 (C), 98.59 (C), 126.61 (2CH), 126.85 (2CH), 126.92 (CH), 128.72(CH), 128.93 (2CH), 129.48 (2CH), 132.44 (C), 140.37(C). MS(ESI): M⁺ = 240.0611 (calcd for C₁₅H₁₂OS = 240.0609).

S5. NMR Characterization of Lithium Reagents

Product Lithium Acetylides (4a-d). Lithium acetylide products were characterized by ^{13}C NMR spectroscopy: **4a**, **4b** and **4c** are dimeric in 1:3 THF/Me₂O, displaying well-resolved 1:2:3:4:3:2:1 septets for the carbanion carbon from coupling to two ^7Li nuclei, or a 1:2:3:2:1 quintet for coupling to two ^6Li nuclei (Fig. S-9). Our chemical shift data (Table S-4) are consistent with those of previously reported lithium acetylides,^[S-14a,S-15,S-16a] except that the carbanion carbon of the silyl acetylides have unusually large downfield chemical shifts relative to the protonated counterpart (data for lithium phenylacetylide and propylacetylide are shown for comparison). Silicon substituents are known to increase the acidity of acetylenic protons more than is predicted based on inductive effects alone,^[S-17, S-18] and it is not surprising that the anomaly is also reflected in the NMR spectrum of the anion as well as the kinetics of deprotonation. Acetylide **4d** was monomeric and is the first monomeric lithium acetylide to be characterized by NMR spectroscopy. 3,3,3-Triphenylpropynyllithium was shown to be partially monomeric in THF solution from analysis of the concentration dependence of equilibrium acidities.^[S-19] A metal free “naked” acetylide anion with a phosphazanium (P₄) counterion has been characterized by NMR.^[S-20] Monomeric lithium acetylides have also been observed in the gas phase.^[S-21]

Table S-4. Acetylene and lithium acetylide chemical shifts in 1:3 THF/Me₂O at -125 °C to -135 °C.

R		H-C≡C-R	Li-C≡C-R	Li-C≡C-R	$\delta\Delta C_1$	$\delta_{7\text{Li}}$	$^1J_{\text{C-}^7\text{Li}}$
Me ₃ Si-	(a)	96.8	168.6 (dim)	115.7	71.8	0.35	22 Hz
Ph ₃ Si-	(b)	101.9	176.4 (dim)	109.4	74.5	0.66	20.6 Hz
PhS-	(c)	92.3	156.8 (dim)	84.6	65	0.72	22 Hz
<i>p</i> -Tol-SO ₂ -	(d)	84.1	165 (mon)	102.8	81	-0.28	34 Hz
Ph-		80	139.8 (dim)	113.7	59.8	0.86	21.9 Hz
Pr-		70.8	118.2 (tet)	113.2	47.4	0.65	15.9 Hz

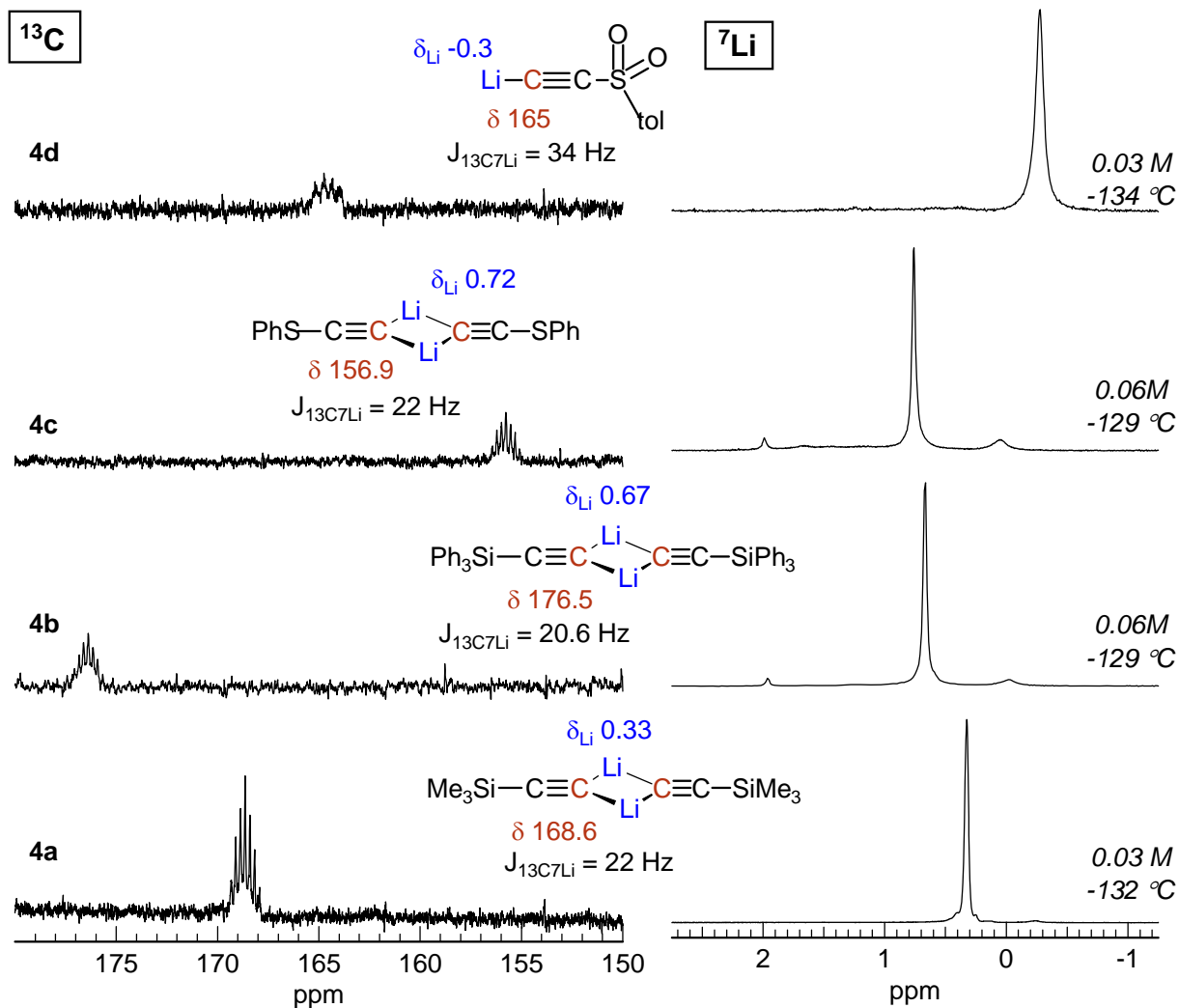


Figure S-9. ^{13}C and ^7Li NMR spectroscopy of lithium acetylides **4a** to **4d** in 1:3 THF/Me₂O.

The mixed dimer is a thermodynamically favored structure that forms in high concentration when one equivalent of *n*-BuLi is added to a solution of the dimeric lithium (trimethylsilyl)acetylide. It can also be prepared by adding 0.5 equiv. of acetylene to a solution of *n*-BuLi (Fig. S-10). The ^7Li chemical shift exactly midway between the homodimers is suggestive of a mixed dimer. Coupling to lithium could not be resolved with ^7Li , however, the ^{13}C NMR spectrum of a ^6Li labeled sample confirmed the dimer assignment as the anionic carbon displayed a 1:2:3:2:1 pentet from coupling to two ^6Li nuclei.

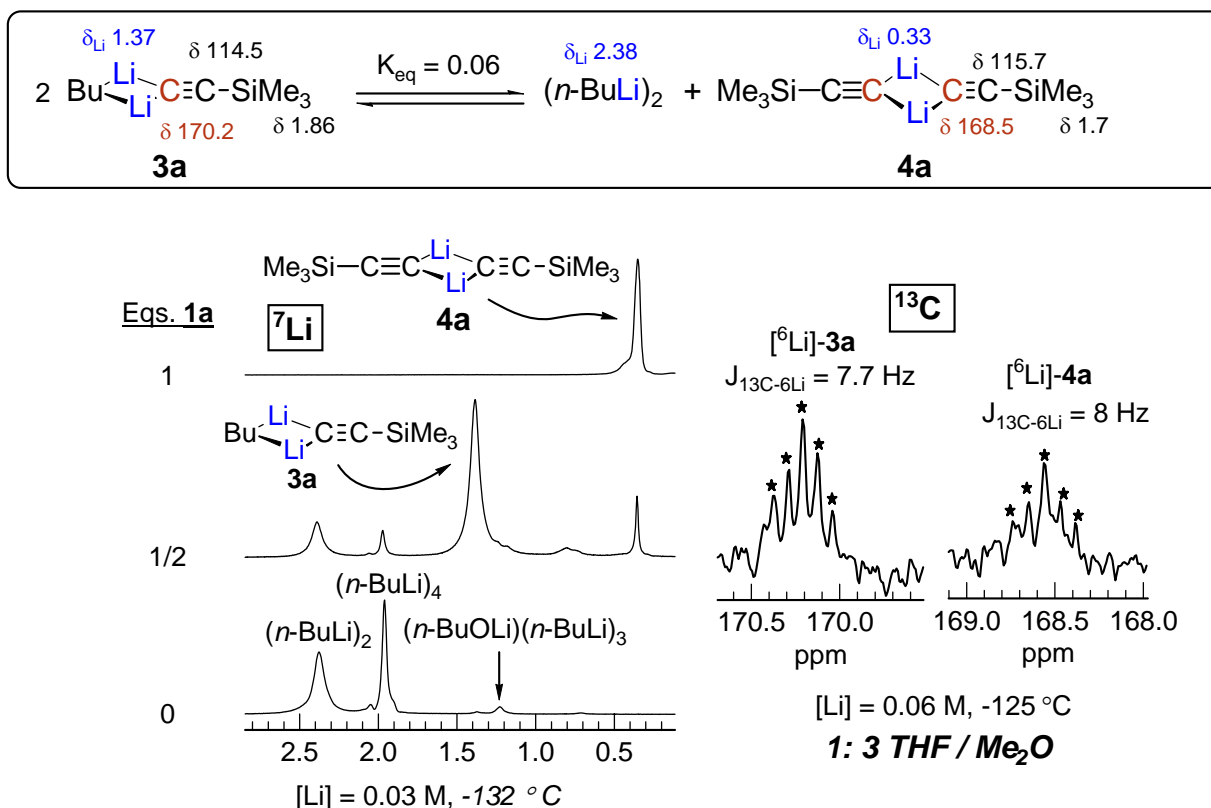


Figure S-10. Spectroscopy of the mixed dimer **4a**, and comparison with the homo-dimers **3a** and $(n\text{-BuLi})_2$.

Recrystallization of 2-Methoxy-6-(methoxymethyl)phenyllithium (5). 2-Trimethylstannyl-3-(methoxymethyl)anisole (0.13 g, 0.41 mmol) was weighed into a N_2 purged NMR tube and dissolved in 1 mL of ether. The sample was cooled in a dry ice/acetone bath and MeLi (0.32 mL, 1.4 M/ether, 0.45 mmol) was added. The sample was allowed to warm slightly, until the solution turned a faint yellow. The sample was then placed back in the dry ice bath for 1-2 min, before placing in a -20°C freezer. Crystals typically formed within 30 min. The ether supernatant was removed by cannula. The crystals were washed with ether (3x1 mL), weighed wet (0.06 g, <0.39 mmol) and dissolved in the desired solvent mixture for NMR spectroscopy.

Characterization of 2-Methoxy-6-methoxymethylphenyllithium (5). Variable temperature NMR in 3:2 THF/ether confirmed the presence of three aggregates and provided estimates for the barriers to interconversion (Fig. S-11). The coalescence temperature by ^7Li NMR spectroscopy for two of the isomers is ca -132°C , which corresponds roughly to a $\Delta G^\ddagger = 7.2$ kcal/mol, an exchange rate that is too high for study by RINMR. The coalescence temperature for exchange with the third isomer is ca -29°C , which corresponds to an estimated $\Delta G^\ddagger = 11.7$ kcal/mol.

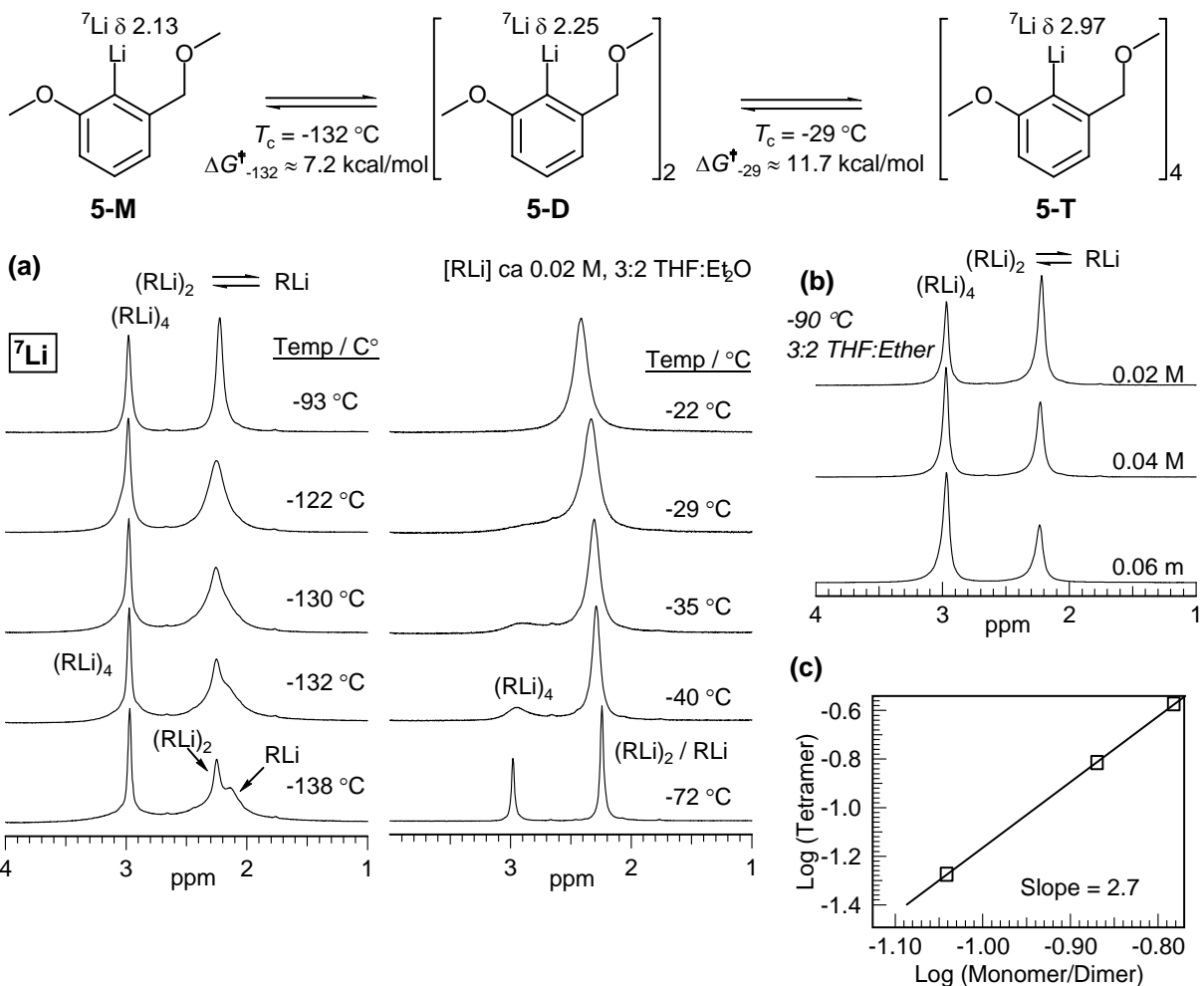


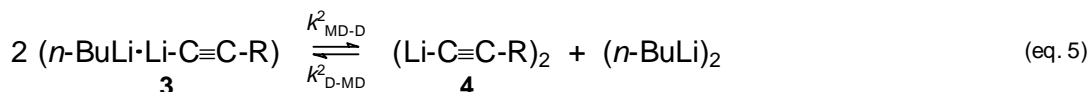
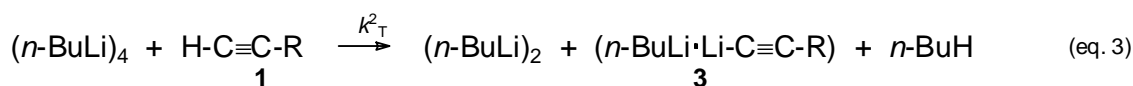
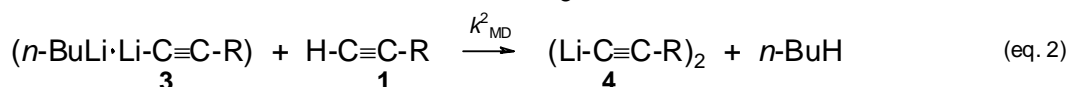
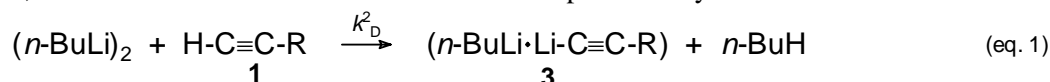
Figure S-11. (a) Variable temperature ⁷Li NMR spectra of 2-methoxy-6-(methoxymethyl)phenyllithium (**5**) in 3:2 THF/ether. (b) ⁷Li NMR study of variable concentration samples. (c) Variable concentration log/log plot.

A variable concentration experiment at -90 °C (Fig. S-11) established that the downfield peak at δ 2.97 ppm in the ⁷Li NMR spectra is the higher aggregate. A plot of log([**5-M**] + [**5-D**]) vs. log[**5-T**] gives a slope of 2.7, as expected for the summation of the expected slope of 4 (monomer vs. tetramer) and 2 (dimer vs. tetramer). The low solubility of the tetramer and the overlap of the two lower aggregates made a more detailed concentration dependence experiment difficult. At concentrations higher than about 0.1 M, the tetramer began to precipitate, so only a very limited range of concentrations could be examined. A more detailed description of the structure will be reported separately.

S6. Rapid Injection NMR Kinetics

Preparation of *n*-BuLi Samples. A 10 mm NMR tube sawed to a length of 18 cm was sealed with a septum, grease, and parafilm, and purged with Argon. The ^{13}C chemical shift thermometer (10% ^{13}C labeled *tris*(trimethylsilyl)methane, 4 μL),^[S-9] an internal standard for concentrations (PhSiMe₃, 28 mg, 0.186 mmol) and substrate (for cases where *n*-BuLi is to be injected) were weighed in, followed by 1 mL of freshly distilled THF. The NMR tube was cooled in a dry ice/acetone bath. Me₂O (~3 mL) is distilled via cannula into the NMR tube from a graduated conical cylinder containing *n*-BuLi (for drying). For cases where substrate will be injected, *n*-BuLi (0.05-0.1 mL, 2.5 M/hexane, 0.13 mmol) was added to the NMR tube.

Kinetic Simulations. For the reactions with *n*-BuLi and acetylenes, rate constants were determined by a least squares fit of experimental and calculated points from numerical integration of the equations in Fig. S-12. For the graphs reporting concentration vs time plots the points are experimental and the lines represent these kinetic simulations. In the ^7Li NMR RINMR experiments with **1** there was no internal integration standard, so concentrations were normalized, assuming that the sum of the signals for (*n*-BuLi)₂, (*n*-BuLi)₄, **3**, and **4** were constant. The products of the reaction of **1** with *n*-BuLi tetramer are unknown. The reasonable process shown in eq. 3 was assumed for convenience in the simulations. Eq. 3 becomes significant only for reactions with **1c**, and here the intermediate **3c** does not build up detectably.



$$K_{\text{MD}} = \frac{k_{\text{MD-D}}^2}{k_{\text{D-MD}}^2} = \frac{[\mathbf{4}] [(n\text{-BuLi})_2]}{[\mathbf{3}]^2}$$

Figure S-12. Kinetic scheme for reactions of *n*-BuLi with acetylenes.

Reactivity of *n*-BuLi with (Trimethylsilyl)acetylene (1a**).** (Trimethylsilyl)acetylene (0.2 mL) was injected at varying concentrations (Fig. S-13 (a) 1 M in 1:1 THF/ether, (b) 2.6 M in 1:1 THF/ether, (c) neat) into a solution of *n*-BuLi (0.03 M) in 4 mL of 1:3 THF/Me₂O. In these experiments $k_{\text{D-1a}}$ is not well defined since most of the dimer reaction occurs during the 1-second mixing period. The temperature was slightly higher than our target of -130 °C in run (a), and slightly lower in run (c), and this fully accounts for the larger values of $k_{\text{MD-1a}}$ and k_T in run (a) and the smaller values in run (c). Because of the temperature variance, the reported value of $k_{\text{MD-1a}}^2 = 2.6 \text{ M}^{-1} \text{ s}^{-1}$ is for the run at -129 °C. The reaction of **3a** with **1a** is thus first order in **1a**. As can be seen in Fig. S-14, the rate of reaction with *n*-BuLi tetramer is zero-order in **1a**, so only eq. 4 is operative and there is no detectable contribution from eq. 3.

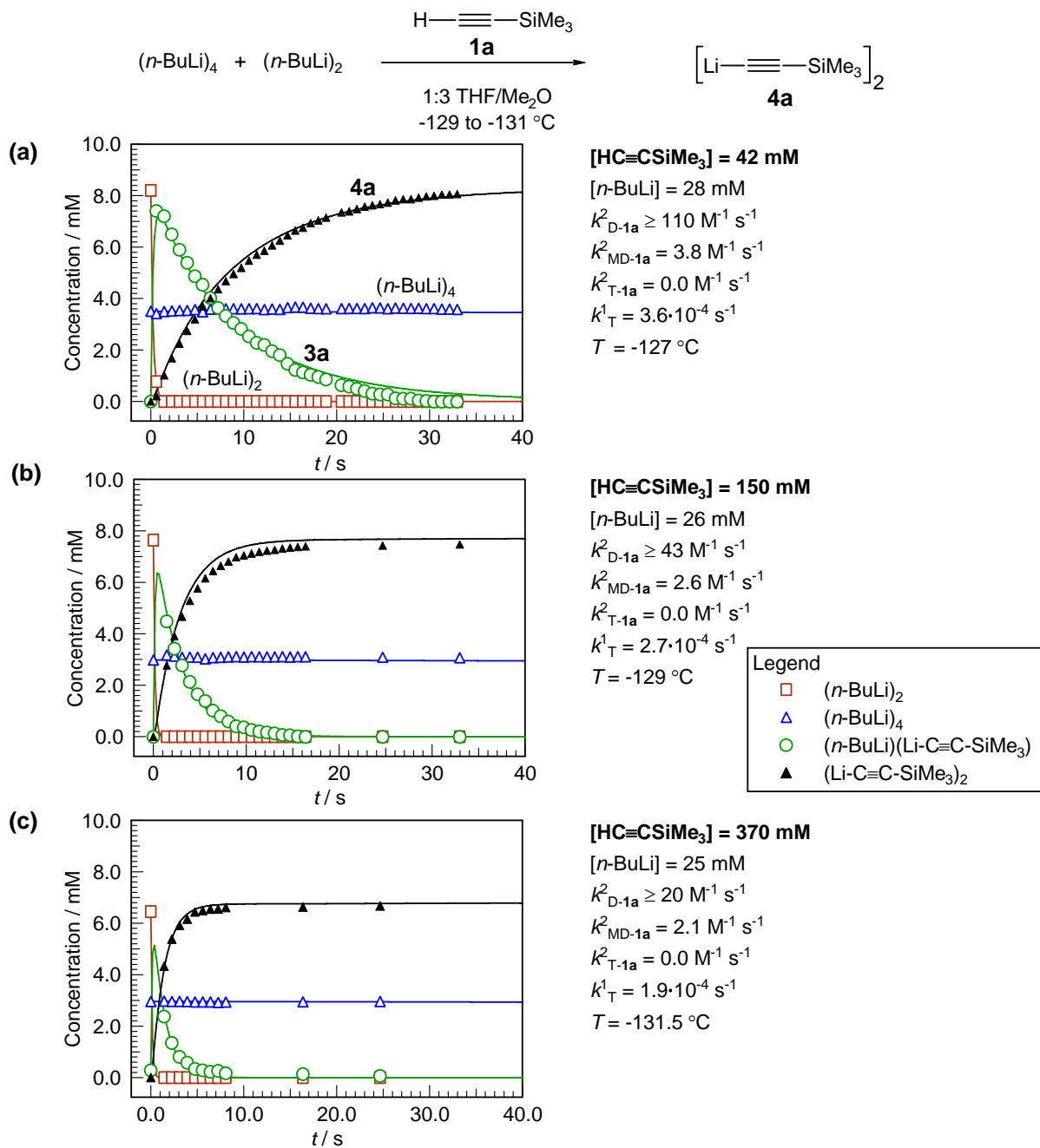


Figure S-13. Time vs. concentration plots and kinetic simulations for 0.2 mL injections of varying concentrations of **1a** in 1:1 THF/ether into 4 mL of a 0.03 M solution of *n*-BuLi in 1:3 THF/Me₂O. The lines are numeric integration simulations using the kinetic scheme of Fig. S-12 and the rate constants shown.

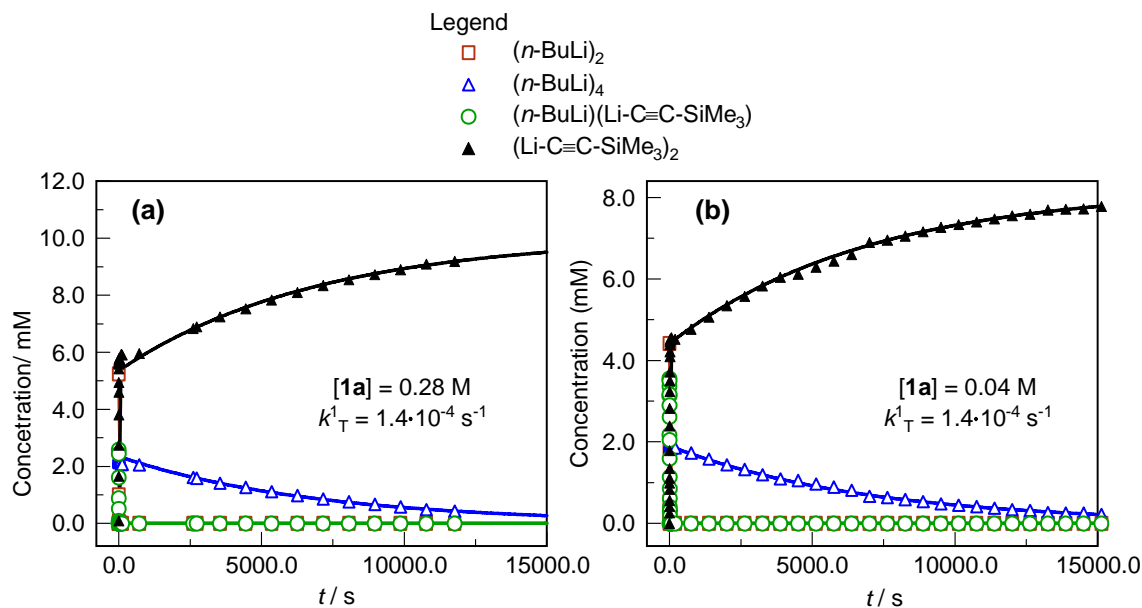


Figure S-14. The injection of (a) 0.2 mL of neat **1a** and (b) 0.2 mL of a 1 M solution of **1a** in 1:1 THF/ether into a 0.03 M solution of *n*-BuLi in 4 mL of 1:3 THF/Me₂O at -135 °C. The lines are numeric integration simulations using the kinetic scheme of Fig. S-12 and the rate constants shown.

Reactivity of *n*-BuLi with *d*-(Trimethylsilyl)acetylene (*d*-1a**).** *d*-(Trimethylsilyl)acetylene was injected (0.2 mL) at varying concentrations (Fig. S-15 (a) 0.9 M in 1:1 THF/ether, (b) 3.8 M in 1:1 THF/ether, (c) NEAT) into a solution of *n*-BuLi (0.03 M) in 4 mL of 1:3 THF/Me₂O. The reaction of *n*-BuLi dimer was first order in *d*-**1a**. The rate of reaction of the mixed dimer **3a** was ca 0.7 order in *d*-**1a**, as reflected by the high $k_{\text{MD-d-1a}}^2$ value in Fig. S-15a, compared to the lower values in Fig. S-15b and Fig. S-15c. This trend was reproducible and implies a competing first order rate determining process (zero order in acetylene, first order in **3a**) such as conversion of mixed dimer **3a** to a very reactive open dimer,^[S-16b] or even to monomers. Rate determining conversion to monomers would appear to be ruled out by the DNMR studies of *n*-BuLi in THF,^[S-14b] where line shape analysis showed that loss of C-Li *J* coupling in the dimer occurred on the same time scale as dimer-tetramer interconversion. Thus, interconversion of *n*-BuLi dimers and monomers (which would result in loss of coupling) is at least 3 orders of magnitude slower than the reactions of the dimer and mixed dimer with **1a** and *d*-**1a**.

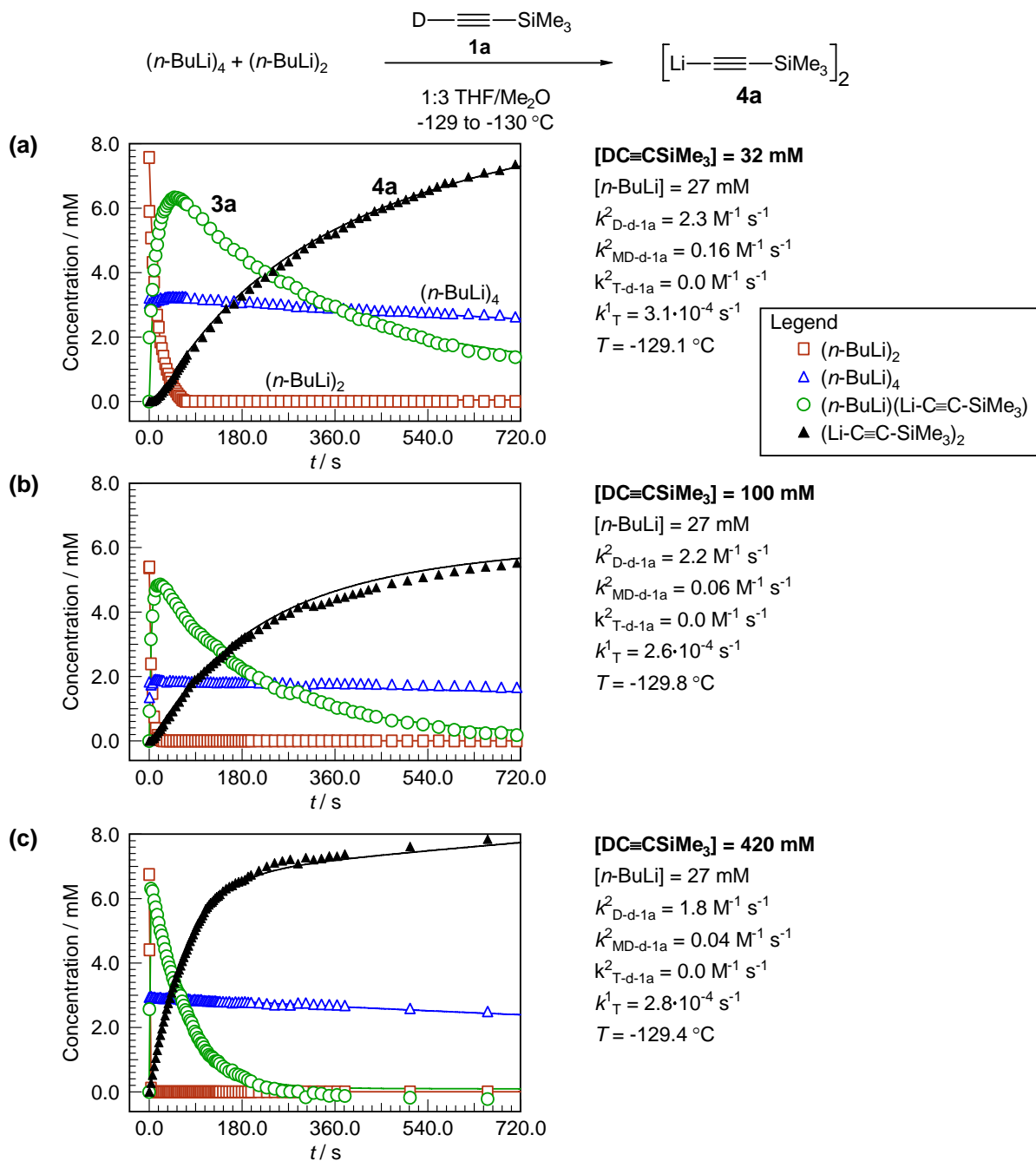


Figure S-15. Time vs. concentration plots and kinetic simulations for 0.2 mL injections of varying concentrations of *d*-(trimethylsilyl)acetylene into a 0.03 M solution of *n*-BuLi in 4 mL of 1:3 THF/Me₂O at ca -129 °C. The lines are numeric integration simulations using the kinetic scheme of Fig. S-12 and the rate constants shown. The value of $k_{\text{D-d-1a}}^2 = 2.1 \text{ M}^{-1} \text{ s}^{-1}$ reported in the main body of the paper, is an average of the three trials. The value of $k_{\text{MD-d-1a}}^2 = 0.04 \text{ M}^{-1} \text{ s}^{-1}$ was used in the main body of the paper, since for that trial the main contribution to the rate is the mixed dimer reacting directly.

Disproportionation of the Mixed Dimer 3a. The disproportionation of **3a** to $(n\text{-BuLi})_2$ and **4a** (eq. 5 in Fig. S-12) provides an alternative path for the reaction of mixed dimer **3a** with **1a** that is zero order in acetylene. We estimated the rate of this process as follows. The rate constant for comproportionation of **3a** ($k_{\text{D-MD}}^2$, eq. 5) was measured by injecting a solution of the acetylide homodimer **4a** into a solution of $n\text{-BuLi}$ (Fig. S-16), giving $k_{\text{D-MD}}^2 = 2.7 \text{ M}^{-1} \text{ s}^{-1}$ (we did not prove the kinetic form of this process but assume that it is second order and follows eq. 5). From this rate constant and the measured equilibrium constant $K_{\text{MD}} = 0.06$ (Fig. S-10) we can calculate $k_{\text{MD-D}}^2 = 0.15 \text{ M}^{-1} \text{ s}^{-1}$ (rate constant for the reverse reaction, disproportionation). Disproportionation does not compete with eq. 2 for the protio substrate **1a**, since a calculated k_{obs} (from $k_{\text{MD-D}}^2$ and $[\mathbf{3a}]$) under the conditions of the experiment in Fig. 13a is 0.0011 s^{-1} , whereas k_{obs} for the reaction of **3a** with **1a** is 0.10 s^{-1} , a factor of 100 larger. This is consistent with the observation that reaction of **3a** was first order in **1a** (competitive disproportionation of **3a** would result in a lower order in **1a**). On the other hand, for the deuterated substrate **d-1a**, which is 1/40 as reactive as **1a**, the disproportionation starts to become competitive at the lowest concentration of **d-1a** ($k_{\text{obs}} = 2.6 \cdot 10^{-4} \text{ s}^{-1}$ for disappearance of **3a**, Fig. S-15a), but contributes at most 20%-30% to the rate. Second order disproportionation may be in part responsible for the lower order in acetylene (0.7) found for the deuterated substrate. It cannot be entirely responsible, since a significant contribution from Eq. 5 does not provide a satisfactory fitting of the experimental and simulated rate plots for Fig. S-15a.

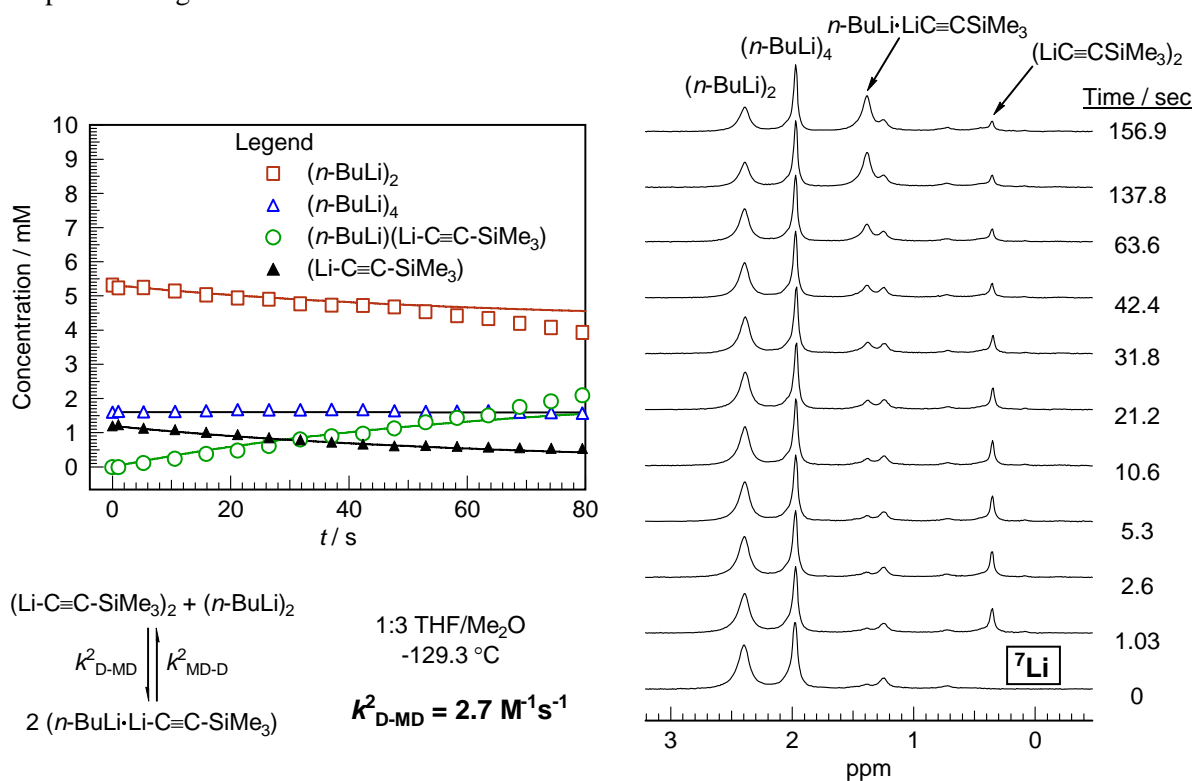


Figure S-16. A solution of lithium (trimethylsilyl)acetylide (0.2 mL, 0.22 M in THF) was injected into a 0.022 M solution of $n\text{-BuLi}$ in 4 mL of 1:3 THF/Me₂O at $-129.3 \text{ }^\circ\text{C}$. $k_{\text{D-MD}}^2$ was determined by kinetic simulation of initial rates.

Reactivity of (*n*-BuLi)₄ with (Phenylthio)acetylene (1c). *n*-BuLi (0.08 mL, 2.5 M/hexanes) was injected into a solution of (phenylthio)acetylene (0.06-0.75 M) in 4 mL of 1:3 THF/Me₂O at ca -129 °C (Fig. S-17). The initial concentration of acetylene was determined using *tris*(trimethylsilyl)methane as an internal concentration standard (in addition to its use as a shift thermometer^[S-9]). Since these are “inverse mode” injections (section S1, Fig. S-7), neither the dimer nor the mixed dimer build up observably. For the simulation, k^2_{D-1c} and k^2_{MD-1c} were both set to an arbitrary large number ($\geq 5 \text{ M}^{-1} \text{ s}^{-1}$). The rate constant used for dissociation of the tetramer to the dimer (k^1_T) was based upon experiments with other acetylenes where dissociation was shown to be the rate limiting step.

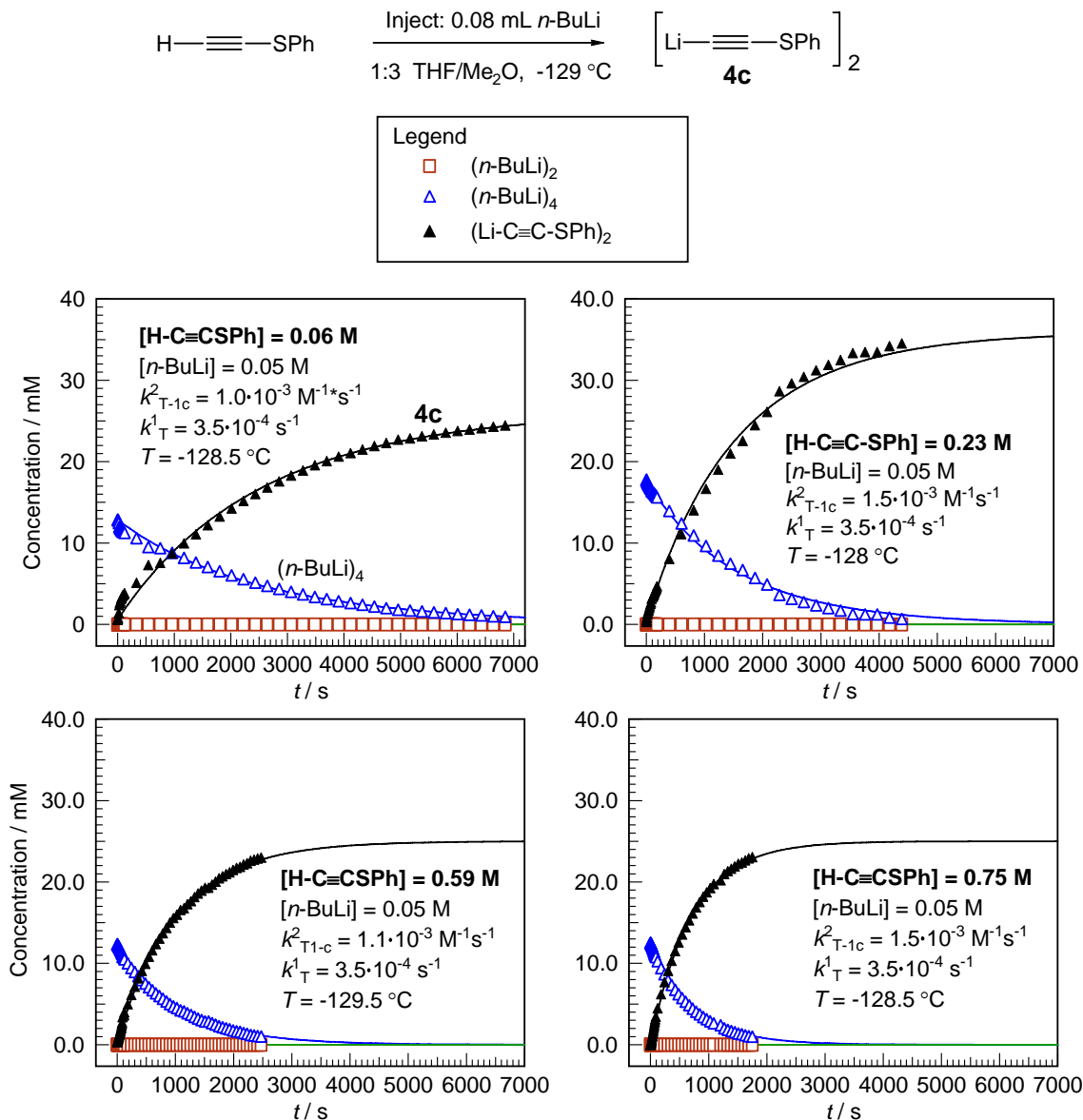


Figure S-17. Time vs. concentration plots and kinetic simulations for 0.08 mL injections of *n*-BuLi (2.5 M hexanes) into varying concentrations of (phenylthio)acetylene in 4 mL of 1:3 THF/Me₂O at ca -129 °C. The value of $k^2_{T-1c} = 1.3 \cdot 10^{-3} \text{ M}^{-1} \text{ s}^{-1}$ reported in the main body of the paper is an average of the four trials.

Reactivity of (*n*-BuLi)₄ with Benzaldehyde. Benzaldehyde was injected (0.3 mL neat or 0.17 mL of a 1.3 M solution in ether) into a solution of *n*-BuLi (0.04-0.06 M) in 4 mL of 1:3 THF/Me₂O (Fig. S-18). The slightly less than first order dependence (*n* = 0.83) is consistent with the known rate of the competing first order process, dissociation of *n*-BuLi tetramer to dimer. The dimer reacts faster than can be measured.

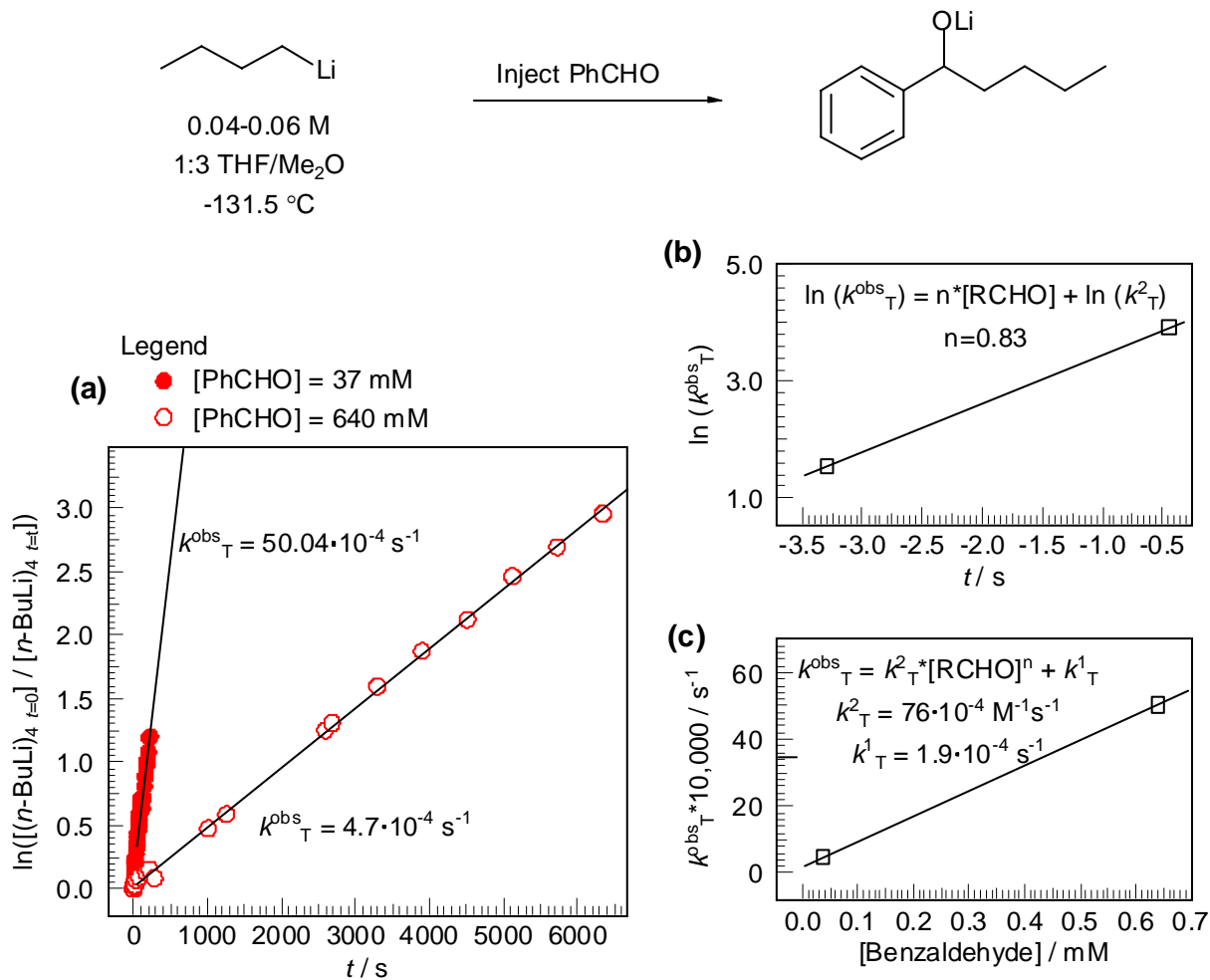


Figure S-18. (a) First order rate plots for reaction of (*n*-BuLi)₄ with benzaldehyde. (b) Determination of order in aldehyde. (c) Determination of the first and second order components.

Reactivity of $(n\text{BuLi})_4$ with p -Diethylaminobenzaldehyde. p -Diethylaminobenzaldehyde (Fig. S-19 (a) 1.8 M in 3:2 THF/Et₂O and (b) 6.3 M in 4:1 THF/Et₂O) was injected into a solution of n -BuLi (0.08 M) in 4 mL of 1:3 THF/Me₂O at -127.5 °C.

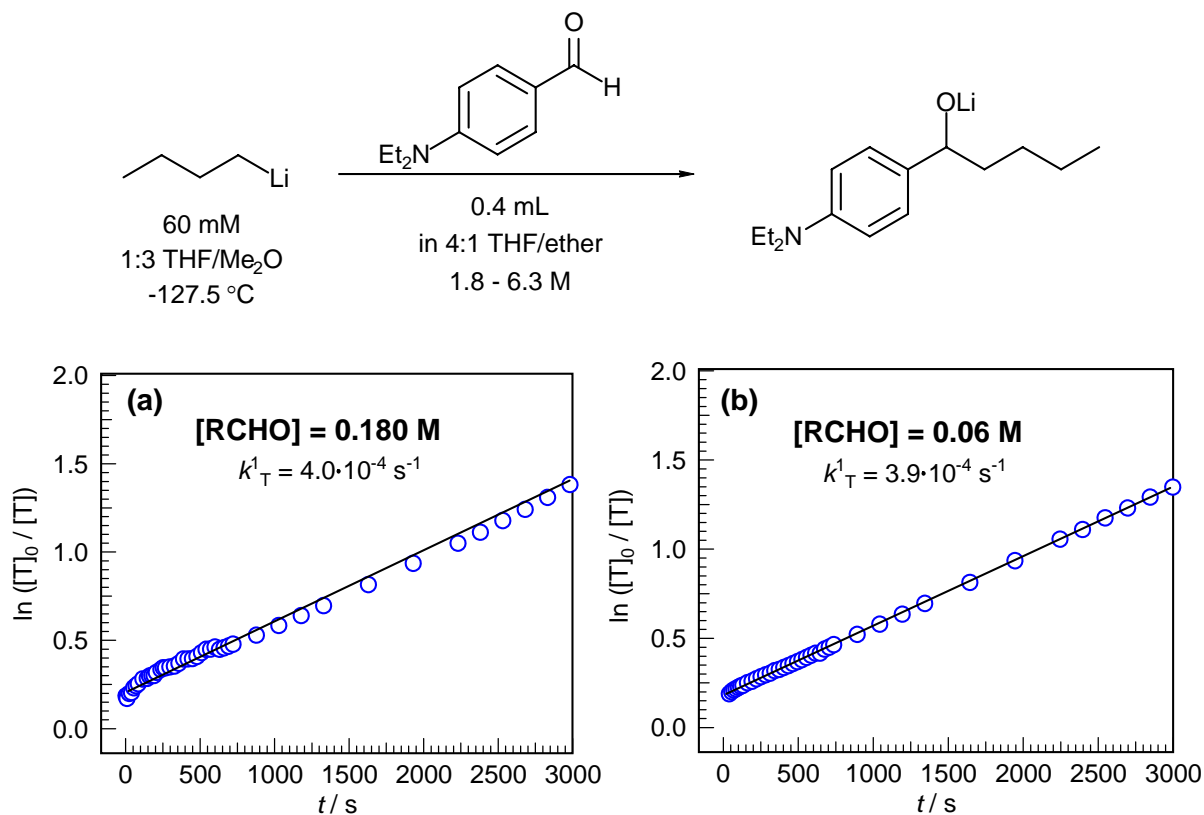


Figure S-19. First order plots of the reaction of $(n\text{-BuLi})_4$ with p -diethylaminobenzaldehyde.

Reactivity of 2-Methoxy-6-(methoxymethyl)phenyllithium with *d*-1a and *1d*. *d*- (Trimethylsilyl)acetylene was injected (0.1 mL) as a solution in 1:1 THF/ether (0.5 M or 2 M) into a 0.01 M solution of **5** in 3:2 THF/ether at -128 °C. A k_{M-d-1a}^{obs} for two runs was determined based on the method of initial rates. A plot of $[d-1a]$ vs. k_{M-d-1a}^{obs} gave an estimated $k_{M-d-1a}^2 = 0.61 \text{ M}^{-1} \text{ s}^{-1}$, while $\ln[d-1a]$ vs. $\ln(k_{M-d-1a}^{obs})$ indicated the reaction is within error of first order in acetylene (Fig. S-20).

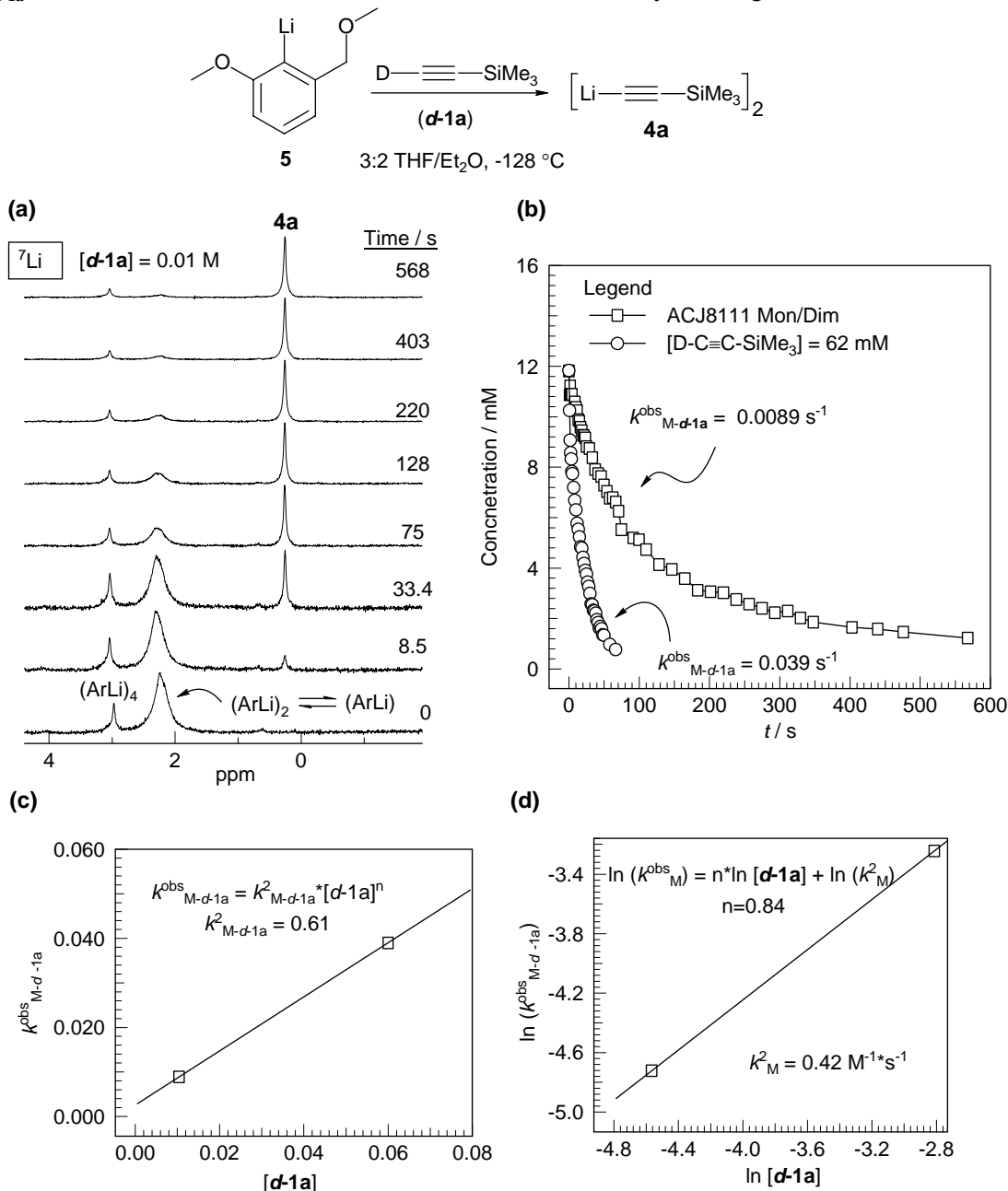


Figure S-20. The reaction of 0.01 M **5** with 0.01 M and 0.05 M *d*-1a in 3:2 THF/ether at -128 °C. (a) RINMR stacked plot for injection of *d*-1a into a solution of **5**. (b) Raw rate plots for two concentrations of *d*-1a. (c) Initial rate plot vs concentration. (d) Ln-ln plot to determine order in *d*-1a.

A solution of (*p*-tolylsulfonyl)acetylene (0.2 mL, 1.9 M in 5:3 THF/ether or 5.7 M in THF) was injected into 3 mL of a 0.04 M solution of **5** in 3:2 THF/ether at -127 °C. The rate of tetramer reacting with **1d** was independent of the concentration of acetylene ($k_T^1 = 2.2 \cdot 10^{-5} \text{ s}^{-1}$) indicating the tetramer must first dissociate before reacting (Fig. S-21).

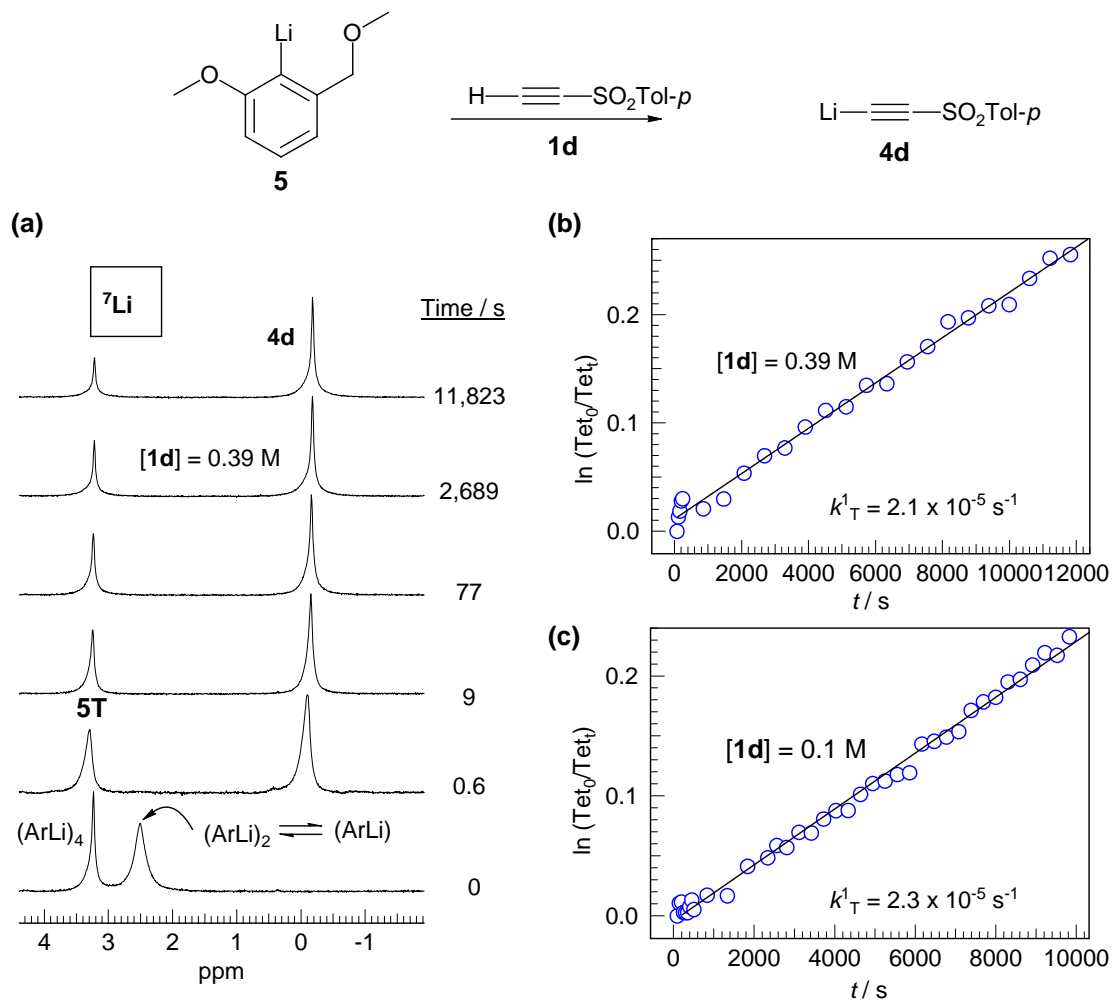


Figure S-21. (a) Injection of 5.7 M solution of **1d** in 5:3 THF/ether (0.23 mL, 0.41 M *in situ*) into a solution of **5** (0.04 M) in 3:2 THF/ether at $-127\text{ }^{\circ}\text{C}$. (b) & (c) Kinetic plots of tetramer disappearance for two concentrations of **1d**, showing reaction is zero order in acetylene ($k^2_{\text{T}} < 5.1 \cdot 10^{-5} \text{ M}^{-1} \text{ s}^{-1}$). Concentrations are adjusted to reflect the amount of **1d** remaining after the monomer and dimer react.

S8. References Supporting Information

- [S-1] (a) McGarrity, J. F.; Prodolliet, J.; Smyth, T. *Org. Mag. Res.* **1981**, *17*, 59-65. (b) McGarrity, J. F.; Ogle, C. A.; Brich, Z.; Loosli, H. R. *J. Am. Chem. Soc.* **1985**, *107*, 1810-1815.
- [S-2] (a) Schleyer, P. v. R.; Bauer, W. in: V. Snieckus (Ed.), *Advances in Carbanion Chemistry*, Vol 1, Jai Press, Greenwich, CT, 1992, p. 89 f. The RINMR device description in this review article can be found p. 108 f. Bauer, W. *Analyse* **1986**, *17* (Kontron Co., Munich, Germany). (b) Bauer, W.; Winchester, W. R.; Schleyer, P. v. R. *Organometallics* **1987**, *6*, 2371-2379.
- [S-3] Reetz, M. T.; Raguse, B.; Marth, C. F.; Huegel, H. M.; Bach, T.; Fox, D. N. A. *Tetrahedron*, **1992**, *48*, 5731-5742.
- [S-4] Palmer, C. A.; Ogle, C. A.; Arnett, E. M. *J. Am. Chem. Soc.* **1992**, *114*, 5619-5625.
- [S-5] Geletneky, C.; Foersterling, F. H.; Bock, W.; Berger, S. *Chem. Ber.* **1993**, *126*, 2397-2401.
- [S-6] Denmark, S. E.; Pham, S. M. *Helv. Chim. Acta* **2000**, *83*, 1846-1853.
- [S-7] Bertz, S. H.; Carlin, C. M.; Deadwyler, D. A.; Murphy, M. D.; Ogle, C. A.; Seagle, P. H. *J. Am. Chem. Soc.* **2002**, *124*, 13650-13651.
- [S-8] Mok, K. H.; Nagashima, T.; Day, I. J.; Jones, J. A.; Jones, C. J. V.; Dobson, C. M.; Hore, P. J. *J. Am. Chem. Soc.* **2003**, *125*, 12484-12492.
- [S-9] All temperatures were measured internally using our ¹³C NMR spectroscopic chemical shift thermometer, *tris*(trimethylsilyl)methane: Sikorski, W.S.; Sanders, A.W.; Reich, H. J. *Magn. Resonan. Chem.* **1998**, *36*, S118-S124.
- [S-10] Watson, S. C.; Eastham, J. F. *J. Organomet. Chem.* **1967**, *9*, 165-168.
- [S-11] Herunsalee, A.; Isobe, M.; Goto, T. *Tetrahedron*, **1991**, *47*, 3727-3736.
- [S-12] Makosza, M.; Chesnokov, Alexey A. *Tetrahedron* **2003**, *59*, 1995-2000.
- [S-13] Yamabe, H.; Mizuno, A.; Hiroyuki, K.; Nobuharu, I. *J. Am. Chem. Soc.* **2005**, *127*, 3248-3249.
- [S-14] (a) Haessig, R.; Seebach, D. *Helv. Chim. Acta* **1983**, *66*, 2269-2273. (b) Heinzer, J.; Oth, J. F. M.; Seebach, D. *Helv. Chim. Acta* **1985**, *68*, 1848-1862.
- [S-15] (a) Fraenkel, G.; Pramanik, P. J. *Chem. Soc., Chem. Commun.* **1983**, 1527. (b) Fraenkel, G. *Polym. Prep., Am. Chem. Soc. Div. Polym. Chem.* **1986**, *27*, 132-133.
- [S-16] (a) Thompson, A.; Corley, E. G.; Huntington, M. F.; Grabowski, E. J. J.; Remenar, J. F.; Collum, D. B. *J. Am. Chem. Soc.*, **1998**, 2028-2038. (b) Chadwick, S. T.; Rennels, R. A.; Rutherford, J. L.; Collum, D. B. *J. Am. Chem. Soc.* **2000**, *122*, 8640-8647.
- [S-17] Eaborn, C.; Skinner, G. A.; Walton, D. R. M. *J. Chem. Soc. B.* **1966**, 989-990.
- [S-18] Kresge, A. J.; Pruszynski, P.; Stang, P. J.; Williamson, B. L. *J. Org. Chem.* **1991**, *56*, 4808-4811.
- [S-19] Gareyev, R.; Streitwieser, A. *J. Org. Chem.* **1996**, *61*, 1742-1747.
- [S-20] Tanaka, Y.; Arakawa, M.; Yamaguchi, Y.; Hori, C.; Ueno, M.; Tanaka, T.; Imahori, T.; Kondo, Y. *Chem. Asian J.* **2006**, *1*, 581-585.
- [S-21] Grotjahn, D. B.; Apponi, A. J.; Brewster, M. A.; Xin, J.; Ziurys, L.M. *Angew. Chem. Int. Ed.* **1998**, *37*, 2678-2681.